

1. INTRODUCTION

Prestressing, a powerful technique in Civil Engineering, can be defined as the application of a predetermined internal force to a structural member in such a manner that the combined internal stresses in the member, resulting from this force and from external loading, will be confined within specific limits. Whether prestressing is applied to steel or concrete, its ultimate purpose is twofold: first, to induce desirable strains and stresses in the structure and second, to counterbalance undesirable strains and stresses.

The term *pre-tensioning* is used to describe any method of prestressing in which the tendons are tensioned before the concrete is placed. In contrast, *post-tensioning* is a method of prestressing where the tendon is tensioned after the concrete has hardened or—as in this case-study—the steel structural element is built. Post-tensioning offers a means of prestressing on the job site.

When post-tensioning short members, the elongation of the tendon—during the stressing—is small, and requires very precise measurement by the workmen. This is why *bars* are preferred to *cables* as short tendons for post-tensioning. In this example, some frames of a steel structure were post-tensioned with high-strength alloy steel bars.

The bars, once stressed, remain as such forever. Under these high stresses—about 780 MPa or 0.6 uts (ultimate tensile stress)—they are very susceptible to small damage. Surface scratches, cracks, pits or notches, that will not usually affect the performance of bars of concrete reinforcement may become dangerous when present in prestressed bars. In fact, the fractures reported in this paper happened at loads as low as 0.3 uts and were triggered by very small surface cracks.

The purpose of this paper is to illustrate this fact. Two failures of post-tensioning bars with surface damage are analyzed using the tools of Fracture Mechanics and some procedures, based on the concept of *damage tolerance*, are suggested to avoid similar accidents.

2. CASE STUDY: FAILURE OF PRESTRESSED BARS

2.1. *Background*

The reported failures occurred in a prestressed steel structure. To improve the transversal stiffness in some steel frames, post-tensioning with a couple of bars was applied diagonally, as shown in Fig.



Fig. 1. Prestressed steel frame using two bars.

1. The tendons were high strength steel bars, 36 mm diameter, with a rupture load $F_R = 1300$ kN. The chemical composition and mechanical properties of the steel bars are shown in Tables 1 and 2, respectively.

Two fractures happened during building erection when stressing the bars; one at 400 kN (about $0.3F_R$) and another at 600 kN (about $0.46F_R$); both failure loads were well below the scheduled working load of $0.6F_R$.

Examination of the fracture surfaces revealed that in both cases the fracture was triggered by a small surface crack. The morphology of the fracture surfaces was very similar in the two bars; a representative picture is shown in Fig. 2. Observation by scanning electron microscopy revealed a quasi-cleavage morphology.

Table 1. Chemical composition of the steel bars

Element	C	Si	Mn	P	S	V
Weight %	0.65	0.70	1.20	0.014	0.018	0.25

Table 2. Mechanical properties

Elastic modulus	Yield stress	Tensile stress	Elongation under max. load
208 GPa	1143 MPa	1285 MPa	6.7%



Fig. 2. Fracture surface of a broken bar.

2.2. Failure analysis

The fact that fracture was triggered by a surface crack, and also the brittle aspect of the fracture surfaces, suggested linear elastic fracture mechanics as the simplest tool to analyze the failures. To this end the fracture toughness of the bars was measured, the stress intensity factors for the surface cracks were computed and all these results were compared with the available information on the failed bars.

2.2.1. Fracture toughness. Fracture toughness was measured following standards ASTM E 399 [1] and ASTM E 1304 [2], and the two results were almost the same. Standard Single Edge Bend Specimens (SEBS), with 16 mm thickness, were used according to ASTM E 399, and short bar specimens, of 19.5 mm thickness, according to ASTM E 1304. Figure 3 shows the geometry of these samples and the position of the bar from which they were extracted; in both samples the crack plane was transversal to the bar axis in order to reproduce the same propagation plane as in the failed bars.

Experimental results are shown in Table 3. No more tests were performed in view of the small scattering in the recorded toughness values. The small values ($K_{IC} = 33\text{--}35 \text{ MPa m}^{1/2}$) are indicative of brittle behaviour. Two additional test results—load vs COD (Crack Opening Displacement)—from each type of sample, corroborate this supposition.

Figure 4(a) is a typical example of the load–COD records from notched beams. The unloading branch shows successive failures until the broken sample is split in two halves. This behaviour is characteristic of a quasi-stable brittle fracture, where energy absorption is almost constant. To check this hypothesis the *iso-K* curve—corresponding to $K_{IC} = 35 \text{ MPa m}^{1/2}$ —was drawn on Fig. 4(a). It fits extremely well with the unloading branch, adding further support to the use of Linear Elastic Fracture Mechanics. The *iso-K* curve was computed from the stress intensity factor, K_I , and compliance, COD/P, expressions given in Ref. [3], i.e.:

$$K_I = \frac{4P}{B\sqrt{W}} f\left(\frac{a}{W}\right) \quad (1)$$

and

$$\frac{\text{COD}}{P} = \frac{24}{BE} g\left(\frac{a}{W}\right), \quad (2)$$

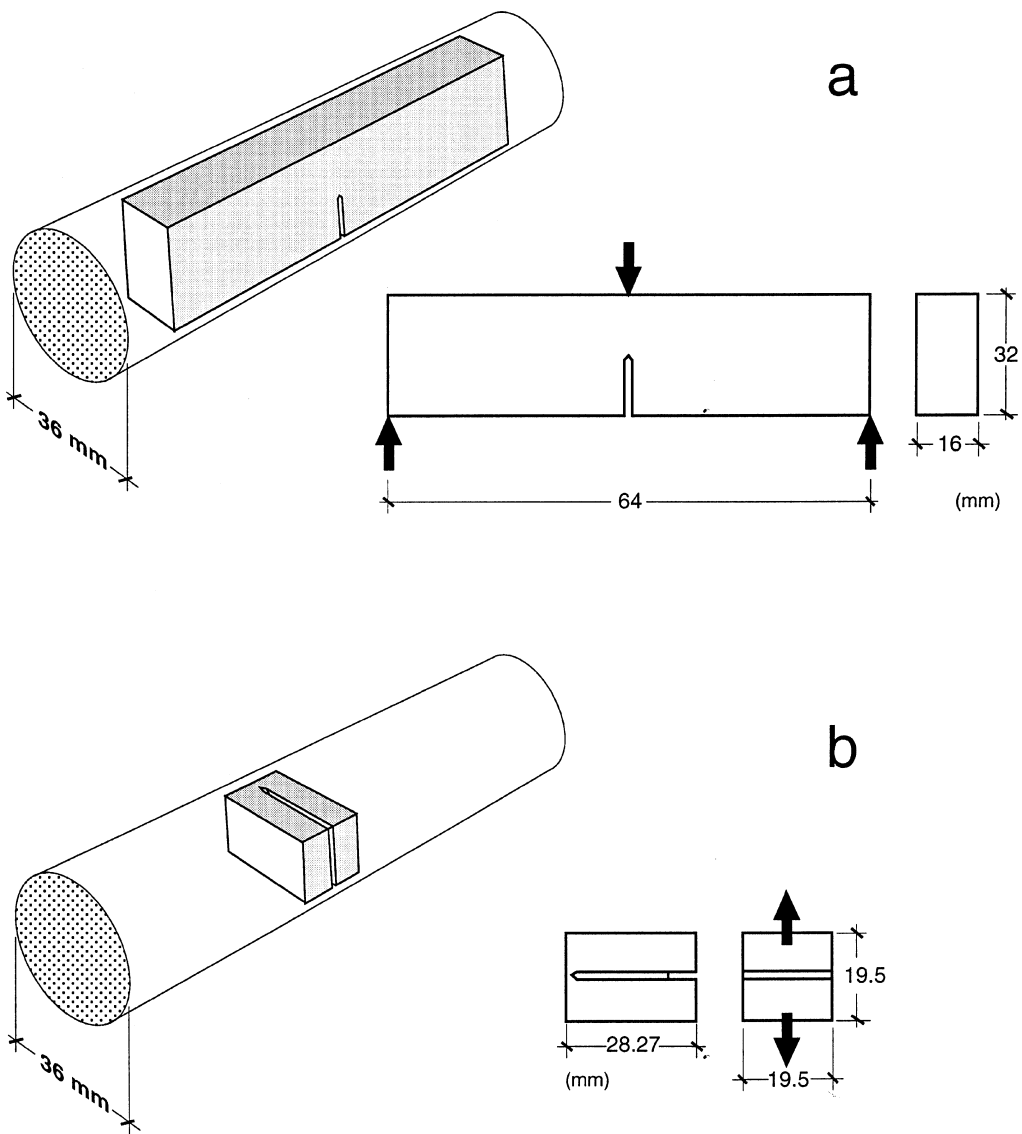


Fig. 3. Test samples for fracture toughness measurement. (a) Notched beams according to ASTM E 399. (b) Short bars according to ASTM E 1304.

Table 3. Fracture toughness K_{IC} (MPa m $^{1/2}$)

Beam	ASTM E 399	32	33	33
Short bar	ASTM E 1304	35	35	36

where P is the applied load, E the elasticity modulus, B , W and a are, respectively, the specimen thickness, width and crack size, and $f(a/W)$ and $g(a/W)$ are non-dimensional functions given in [3]. The *iso-K* curve is the P -COD curve [eqn (2)] after replacing a from eqn (1) with $K_I = K_{IC}$.

Figure 4(b) is also a typical load-COD record obtained from short bar specimens. Crack propagation is stable and proceeds stepwise until reaching the maximum load. Qualitatively, this is the kind of record one should expect for a brittle material with a fracture criterion based on a unique value of fracture toughness rather than a R -curve.

2.2.2. *Stress intensity factor.* The initial surface cracks of the two broken bars were modelled as

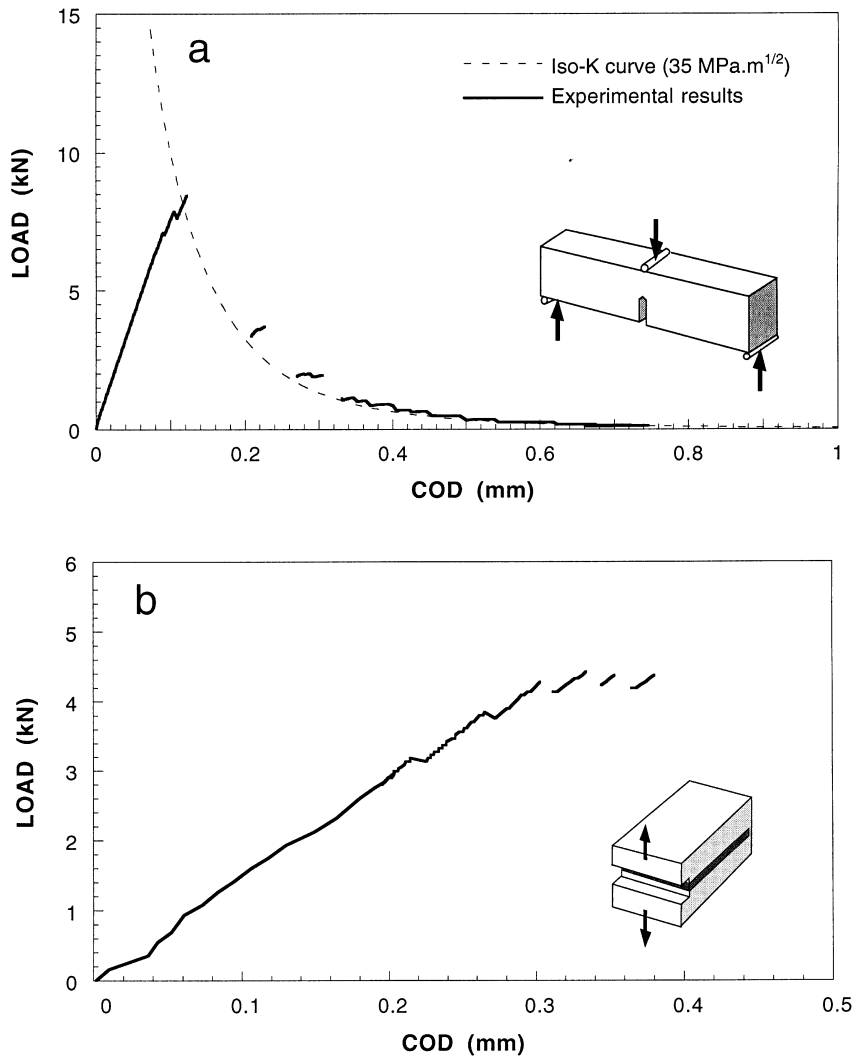


Fig. 4. Load vs crack opening displacement records. (a) Notched beams. (b) Short bars.

elliptical cracks, as sketched in Fig. 5 (a and b are the ellipse semi-axes). The stress intensity factor for this geometry was numerically computed in 1976 by Astiz [4, 5] and also by photoelastic techniques by the authors [6]. When $b > a$ the maximum stress intensity factor is at point A (see Fig. 5) and its value can be expressed as

$$K_I = \frac{4P}{\pi D^2} \sqrt{\pi a} \sum_{i=0, i \neq j}^4 \sum_{j=0}^3 C_{ij} \left(\frac{a}{D} \right)^i \left(\frac{a}{b} \right)^j, \quad (3)$$

where P is the applied load and D is the bar diameter. The coefficients C_{ij} are given in Table 4. A

Table 4. Values of C_{ij}

C_{ij}	$j = 0$	1	2	3
$i = 0$	1.118	-0.179	-0.339	0.130
$i = 2$	1.405	5.902	-9.057	3.032
$i = 3$	3.891	-20.370	23.217	-7.555
$i = 4$	8.328	21.895	-36.992	12.676

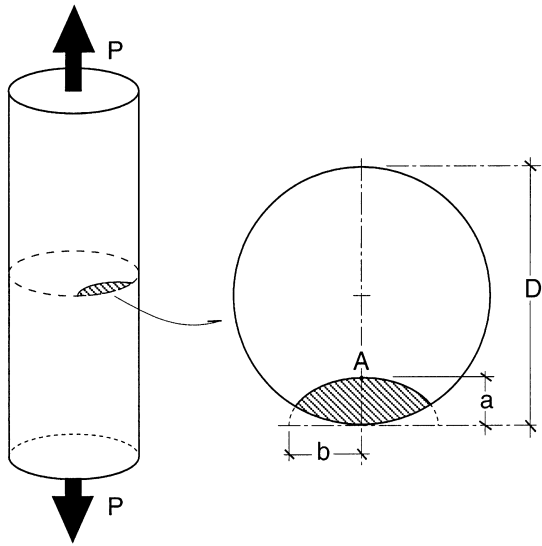


Fig. 5. Geometry and notation of the surface crack.

recent paper on this subject [7] provide more general expressions but the one given above is accurate enough for our purposes.

2.2.3. Rupture load. When Linear Elastic Fracture Mechanics is applicable, the rupture load can be deduced from

$$K_I(P, a, \text{geometry}) = K_{IC}. \quad (4)$$

Taking into account (3), the rupture load is given by:

$$P = \frac{D\sqrt{\pi D}}{4} K_{IC} \cdot M\left(\frac{a}{D}\right), \quad (5)$$

where the non-dimensional function $M(\xi)$ for small values of a/b (as in the considered examples) can be approximated by

$$M(\xi) = \xi^{-1/2} \cdot (1.0806 + 0.6386\xi - 2.4445\xi^2 + 13.463\xi^3)^{-1}. \quad (6)$$

2.2.4. Comparison with failure data. Figure 6 gives the rupture load P as a function of crack depth, a , for $D = 36$ mm and $K_{IC} = 33$ MPa · m^{1/2}. Failure of the two prestressed bars happened at loads of 600 and 400 kN with corresponding crack depths of 0.92 and 1.50 mm. These two rupture data are drawn in Fig. 6. As can be seen there is an excellent agreement with theoretical predictions.

Two more rupture data of bars from the same batch, with small surface cracks similar to the reported ones, are also drawn in Fig. 6 and show the same good agreement. These additional data are experimental results of fracture tests with two precracked bars under axial tension. Precracking was achieved by fatigue using a three point bending assembly and a shallow starter notch with a straight front. Examination, after testing, of the two kinds of cracks—the service and laboratory cracks—showed no difference.

The low values of the bar fracture toughness and the crack-life surface defects allowed a failure analysis based on Linear Elastic Fracture Mechanics. The good agreement with experimental results and theoretical predictions gives further support to this working hypothesis.

3. DESIGN IMPLICATIONS

3.1. Damage tolerance

The analyzed failures reveal the importance of small surface cracks and provide a means of improving the performance of the prestressing bars when such damage may appear. The bars will

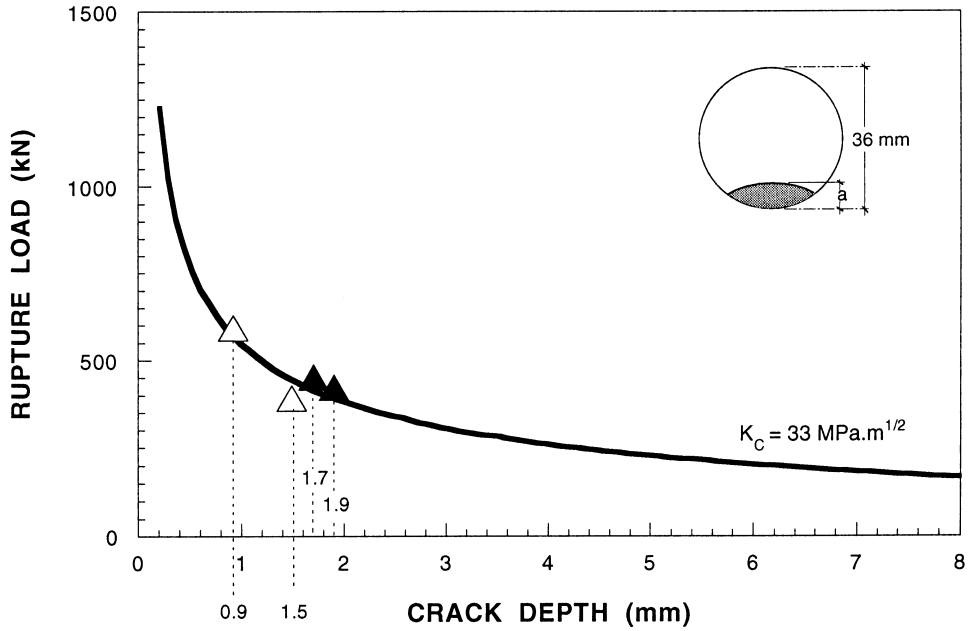


Fig. 6. Rupture load of a cracked bar as a function of crack depth (for $D = 36$ mm and $K_{IC} = 33$ MPa m $^{1/2}$). (\triangle), Actual cracks. (\blacktriangle), Fatigue cracks (laboratory).

be more damage tolerant if their fracture toughness is increased. A simple example illustrates this statement: consider what would happen if higher toughness bars were to sustain the recorded rupture loads— $0.46F_R = 600$ kN and $0.30F_R = 400$ kN. This situation is depicted in Fig. 7(a): if the fracture toughness were 60 MPa m $^{1/2}$ instead of 33 MPa m $^{1/2}$, the critical depth of a surface crack would be about 2.6 and 5.4 mm for 600 and 400 kN, respectively, while for $K_{IC} = 100$ MPa m $^{1/2}$ these figures rise to 6.4 and 10.6 mm. All these values are quite unrealistic for surface cracks, compared to the figures of about 1 mm measured in the broken bars. Higher toughness improves damage tolerance.

Damage due to cracks is much more dangerous than other kinds of damage, such as pits or notches. This was confirmed by testing several bars with artificial notches (the bars came from the same batch as the two broken bars). The results are shown in Fig. 7(b). Notches are not so sharp as cracks, since the curvature radius at the tip of a notch is finite. Artificial notches used in these tests had tip radii of 0.08 and 0.5 mm (see insert in Fig. 7(b)), giving a local stress increase, but not so high as in cracks. Experimental results depicted in Fig. 7(b) show that, for the same depth, cracks are more dangerous than notches, and notch performance is better the higher the tip radius. A review of brittle fracture of steel bars due to cracks or notches, a low temperatures or under high strain rates, is given in Ref. [8].

Figure 7 shows that brittle fracture prediction, the curve for $K_{IC} = 33$ MPa m $^{1/2}$, is a lower envelope for the failure load of a surface damaged bar. A higher envelope corresponding to plastic collapse can be easily derived when a perfect plastic behaviour is assumed. The final result for a straight front surface crack ($a/b \approx 0$) is:

$$P = \sigma_y D^2 N(a/D), \quad (7)$$

where σ_y is a suitable yield stress, and the non-dimensional function $N(\xi)$ is given by

$$\begin{aligned} N(\xi) = \frac{\pi}{4} - \frac{1}{4} \arccos(1-2\xi) - \frac{1}{2} \arcsin[2^{2/3}(\xi-\xi^2)] \\ + \frac{1}{2}(1-2\xi)(\xi-\xi^2)^{1/2} + 2^{-1/3}(\xi-\xi^2)^{1/2}[1-2^{4/3}(\xi-\xi^2)]^{1/2}. \end{aligned} \quad (8)$$

Both curves are drawn in Fig. 7(b). Damage in the form of notches lay in between. Quantifying damage due to pits or notches is difficult on account of the many variables involved. Nevertheless,

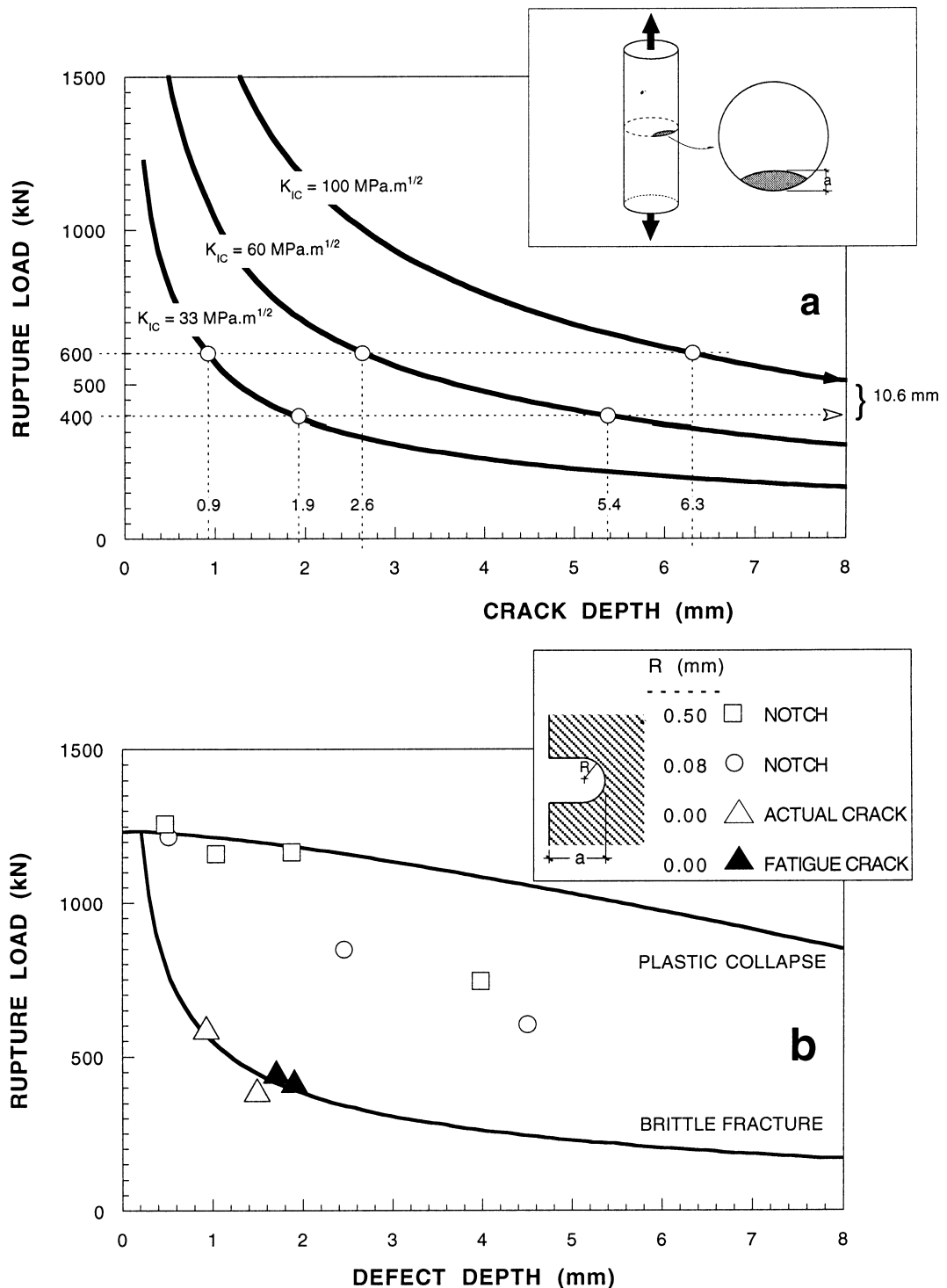


Fig. 7. Damage tolerance diagrams. (a) Cracks: influence of fracture toughness. (b) Notches: influence of tip radius.

Table 5. Critical surface crack depth

Fracture toughness (MPa m ^{1/2})	33	60	100
Critical crack depth (mm)	0.5	1.6	4.1

what appears clearly from the above results is that damage tolerance improves with increased fracture toughness.

549707

1 Background

The article investigates failures of two prestressing tendons, which ruptured at much below specified working load. The tendons were high-strength steel bars 36 mm in diameter and had specified rupture load (F_R) of 1300kN. The working load was specified to be $0,6*F_R$, but the bars fractured at $0,3*F_R$ and $0,46*F_R$.

2 Investigation methods

The failures were investigated with a combination of theoretical evaluation with linear elastic fracture mechanics, and practical experiments.

The fracture surfaces were examined using macroscope and a scanning electron microscope, and both fractures were determined to be quasi-cleavage fractures triggered by a small surface crack.

The chemical composition and mechanical properties of the bars were inspected and found to conform to specification. Tensile strength of was measured to be 1285 MPa, which exceeds the stress that the bars would be subjected to under specified rupture load of 1300 kN (1277 MPa for a Ø36 mm bar). The yield strength was 1143 MPa, which corresponds to a load of 1163 kN, which by far exceeds the loads at which failures occurred. Therefore, linear elastic fracture mechanics was determined to be a suitable tool for analyzing the failures.

The fracture toughness of the material was measured according to ASTM E 399 (notched bars) and ASTM E 1304 (short bars), with samples prepared from tendons from the same manufacturing batch as the failed bars. Both tests produced similar results with values ranging from 32 to 36 MPa \cdot m $^{1/2}$. This is a rather low value, indicating brittle behavior.

In addition to fracture toughness measurements, load versus crack opening displacement (COD) measurements were taken with samples prepared according to the two standards. The results were consistent with quasi-stable cleavage fracture. The crack progressed in a stepwise manner, following iso-K curve ($K_{IC}=35$ MPa \cdot m $^{1/2}$) very closely in the unloading branch of the measurement taken with notched bar specimen, which further supports the use of linear elastic fracture mechanics to investigate the failure.

Computational investigation was done by modelling the fracture-initiating cracks as semi-elliptical surface cracks. First the stress intensity factor K_I was calculated for the modelled cracks, and then rupture load was modelled as a function of crack depth assuming $K_{IC}=33$ MPa \cdot m $^{1/2}$, which corresponds to the fracture toughness measured for the material.

The depths of the failure-initiating cracks were mapped against the computed curve and were found to agree very well with theoretical predictions. To further test the applicability of the linear elastic model, two pre-cracked specimens were prepared by growing fatigue cracks to steel bars from the same manufacturing batch. The specimens were broken in a tensile test, and the fatigue crack depths and rupture loads were also found to correspond very well with the theoretical model.

After verifying that the linear elastic model was accurate for the failure case, effects of crack shape and fracture toughness were investigated computationally. Critical crack depths with higher fracture toughness levels (60 and 100 MPa \cdot m $^{1/2}$) and rupture loads with notches of different tip radius and depth were calculated.

3 Primary cause

The failure was caused by uncontrolled crack propagation under constant load that started from a surface crack in both specimens. The design of the structure called for a very high prestress-

ing load, and subsequently the bars were designed to be loaded to a high fraction of their ultimate tensile strength. As the fracture toughness of the material chosen for the prestressing tendons was relatively low, a situation was created where critical crack length at the design load would have been merely fractions of a millimeter, allowing relatively small defects to develop into catastrophic failures at loading levels significantly below the design load.

4 Alternative mechanisms

As the bars failed during installation, they were not subjected to corrosive environment or cyclic loading, ruling out fatigue and environmentally assisted failure. The temperature likely was not high enough for creep effects to occur either. The article states that the fracture surface was consistent with cleavage fracture under SEM examination but does not provide any images to support this claim. The macroscopic image of the fracture surface, however, does not show any necking or shear lips, which is consistent with brittle failure. Plastic deformation of a bar under tension would result in a “cup and cone” fracture surface, which is not the case here, allowing plastic deformation to be ruled out with relatively high confidence.

5 Preventing further similar methods

The material of the prestressing tendons has too low fracture toughness for the designed loading level, which is a clear design error. It can be corrected by either reducing the loading by increasing the diameter of the bars, or by changing the material to one with higher fracture toughness. However, the fracture toughness would have to increase significantly, as the theoretical predictions calculated in the article show that even with $K_{IC}=60 \text{ MPa}\cdot\text{m}^{1/2}$, the larger crack would have been close to critical length at design load. Fracture toughness in the order of $100 \text{ MPa}\cdot\text{m}^{1/2}$ would be needed to achieve good damage tolerance.

In addition to increasing damage tolerance by lowering the stress or increasing fracture toughness, the prestressing tendons could be inspected before attempting to fully tighten them. As the rupture loads calculated for notches show, the bars are relatively resistant against dents and other visible defects, since even a very sharp notch with tip radius of 0,08 mm could be nearly 3 mm deep before a rupture would occur under the design load. Therefore, ensuring that the bars do not contain cracks is highly important, whereas other defects may be ignored.

Liquid penetrant inspection and magnetic particle inspection are both relatively quick, easy, and effective methods to find surface cracks that are large enough to be potentially critical. Liquid penetrant inspection would be particularly effective if low tension was applied to the bars, and the testing was carried out on-site before full tensioning, as this would open potential cracks, ensuring that the penetrant fluid is able to enter them.

Overall, no single action is sufficient to prevent similar failures from occurring. Instead, the design of the prestressing tendons should be carefully reconsidered. Choosing a material with higher fracture toughness and decreasing the design load relative to rupture load would increase the critical crack depth, and inspecting the bars for potentially critical cracks would prevent similar failures during installation. However, even static structures, especially ones like bridges or high-rise buildings, are subjected to fatigue loading, which could grow the cracks to critical length at design load. Therefore, the entire structure must be designed with adequate redundancy and a periodical inspection program must be implemented to avoid catastrophic failures later within the service life of the structure.

493905

493905

Prestressing is a method used in civil engineering to remove undesirable stresses and strains or introduce desirable stresses and strains in steels or concrete. As such it also makes the material susceptible to small damage like surface scratches and crack pits. Prestressing can be divided into two different methods which are pre-tensioning and post-tensioning. In the analysis prestressed diagonal tendons made of steel bars were used as a case study to study the failure of several tendons which cracked after being post-tensioned. The fractures apparently happened during building erection after being post-tensioned and load was applied to them. The steel bar composition is given but the specific material code is not. The analysis concludes that the fractures happened due to small surface cracks in the tendons.

Several means of investigation were used in the analysis. These include using scanning electron microscopy to study the fracture surface of the broken bar. Using linear elastic fracture mechanics following ASTM standards to calculate fracture toughness. And using computational tools for calculating stress intensity factor K_I for the surface cracks. The chemical composition of the steel and the mechanical properties are given in tables provided in the analysis. However, there is no mention of how accurate these are and if they are just references of literature values. Eventually the results gotten from these investigations were cross referenced with available information of the failed bars.

Using the scanning electron microscopy, a fracture surface of the broken bar was obtained in figure 2. Unfortunately, this is the only fractography provided in the analysis and it shows the surface in low magnification. By using the ASTM standards for test specimens, fracture toughness K_{IC} was obtained which are presented in table 3 of the analysis. The results from the test samples used in the fracture toughness measurements show that the fracture toughness is around 35 MPa in the short bar and around 33 MPa in the beam. The conclusion the analysis has is that the fracture toughness is low enough to be considered to have brittle behavior and it follows the same propagation plane as in the failed bars. In addition to fracture toughness tests, load vs COD test results were also provided in the paper. And iso-K curve was drawn based on the stress intensity factor K_I . The analysis mentions that the iso-K curve fits very well on the load vs COD results drawn in figure 4a. Which would further support their theory of using linear elastic fracture mechanics. Lastly, the analysis obtained rupture load graphs of the cracked bars as a function of crack depth. These graphs show at which point the crack length becomes critical as in the material will have failure. The analysis also concludes based on their information that the damage happened likely due to cracks because pits or notches would not be able to increase the local stress enough to produce a failure under the load, they were in.

The primary cause based on the analysis were the small cracks which have appeared on the steel bars when prestressed. And afterwards when load was applied to the steel bars the material failed in a brittle like mechanism at first. The theory is supported by some of the results. In the single fractography figure, we can see that the top side of the bar is the place where the crack was initiated and propagated. This can be seen as the surface is very flat and likely to be brittle like fracture growth. In the bottom half of the fractography there is more roughness which would indicate a ductile fracture growth. Based on the figure, we can say that it is possible for the material to have had brittle failure at the beginning. And afterwards the material resisted the growth of the crack by a ductile like manner. However, since there are no higher magnification figures of the steel bar it's hard to have a full conclusion on the fracture type. The fracture toughness tests they made with linear elastic fracture mechanics seem to also support their

theory of small surface cracks. The material had lost its fracture toughness property after being prestressed which would indicate that there is some sort of damage in the material. This damage could be caused by notches, pits, or small surface cracks. However, the analysis uses rupture load P data to show that the test specimens used in the case study have similar failure timings as the steel bars when subjected to small surface cracks. In this regard the data supports the theory that there were small surface cracks in the steel bars. The crack initiation was likely caused by small surface crack damage combined with the load. However, the small surface cracks could have also appeared after the loading was applied through fatigue mechanisms. This could be possible if the material was not very high quality, and the load would be enough to cause fatigue damage. This is not discussed in the analysis.

Plastic deformation cannot be ruled out. The material likely had plastic deformation after being subjected to the load. The fractography provided in the analysis shows very much plastic deformation surface at the halfway and bottom parts of the surface.

Creep cannot be ruled out. While highly unlikely to happen in the environment the steel bars are subjected to, there is no mention of the operating temperature and therefore, I wouldn't rule it completely out.

Brittle fracture cannot be ruled out. The fractography does show some flat surface in the top side of the material which does resemble brittle fracture features. In addition, the data provided in the analysis supports that the steel bars had a low fracture toughness which would allow brittle fracture to happen.

Fatigue cannot be ruled out. The steel bars were subjected to loads of 400 kN and 600 kN respectively. These loads can also initiate small surface cracks and afterwards break the material. It is possible for the material to have been poor quality in which fatigue could have happened in these loads.

Environmentally assisted failure cannot be ruled out either. Unfortunately, due to only one fractography which is low magnification, we cannot see the surface very well. One of the best tools for analyzing environmentally assisted failure is to see the fracture surface up close and see whether there are particles or other inconsistencies that shouldn't appear on the material surface. Since we cannot see the material surface up close, we cannot rule out environmentally assisted failure. The steel bars could have had corrosion in the small cracks before the load was applied which would have made them more brittle. Even stress corrosion cracking could be possible.

For future uses of similar steel bars, it would be important to be more precise in the prestressing mechanism. Considering it was likely the reason why the small surface cracks appeared on the material. Other suggestion is to use better steel that is stronger and more resistant for small surface cracks to appear during prestressing. The steel used in the bars was likely AISI 304 or AISI 316 which is a pretty standard steel used in structural materials. However, they are prone to stress corrosion cracking as they are austenitic stainless steels. If stress corrosion cracking happened on the material, then using a better alternative would reduce the risk for failures.



101843742

Materials safety: article exercise

You are working as a materials expert in your organization and your responsibility is to guarantee safe and efficient use of materials in your facility. One day, a failure in similar facility is brought to your attention, and you need to investigate the possible implications this failure has for your facility. Your job is to interpret and analyze the given failure report and to write a report, which will allow others in your organization to understand the key developments and causes leading to the failure and the necessary actions for prevention of such failures.

Read the given article and analyze the failure. Describe, how the deformation and failure mechanisms presented during the course are reflected in the case and establish the chain of actions leading to the failure. The report should work as an introductory material to your team; it should not be very long but it should enable other team members to understand the key features of the failure without reading the failure report itself.

In addition to establishing the primary cause of the failure, show why alternate failure mechanisms can be ruled out. Some failure mechanisms have not been discussed in the course yet. Conduct the analysis using your present knowledge on the subject.

If the author of the failure analysis has, in your view, neglected to address some aspects of the failure, you may indicate this in your report and suggest tests or actions that should have been done to clarify the issue.

Prepare your response by editing this word document and export it as PDF. The file name identifies you and the article. Do not change the file name (other than the extension to pdf). E-mail the pdf to "materials.safety@iikka.fi".

You may use the question list below to guide you in your analysis:

A. Description of investigation methods applied

- **What means of investigation were used in the failure analysis?**

The investigation methods used in the failure analysis included linear elastic fracture mechanics (LEFM) as the primary tool. Surface cracks were modeled as elliptical, and stress intensity factors for these cracks were computed using numerical methods and photoelastic techniques. Additionally, fracture toughness tests were conducted to measure the fracture toughness of the prestressed bars following ASTM standards E 288 and E 0293. Fracture tests were also performed on pre-cracked bars under axial tension to gather additional data.

- **What computational methods were used?**

Computational methods were used to numerically compute stress intensity factors for the elliptical surface cracks. These methods involved mathematical modeling and numerical analysis to determine the critical parameters related to the failure of the prestressed bars.

- **What material or results were obtained?**

The material and results obtained from the investigation included fracture toughness values for the bars, stress intensity factor calculations for surface cracks, and comparisons between theoretical predictions and experimental data. The results demonstrated the critical role of fracture toughness in determining the damage tolerance of prestressed bars and how increased fracture toughness could enhance their performance and resistance to failure.

B. The primary cause of the failure and description of the failure mechanism

- **What is the primary cause of the failure (also provide reasoning)?**

The primary cause of the failure was the presence of small surface cracks in the prestressed steel bars. These cracks, although relatively small, played a critical role in the failure mechanism. The reasoning behind this is that the fracture analysis showed that the bars had low fracture toughness, with a KIC value of $22 \text{ MPa}\cdot\text{m}^{1/2}$. This low fracture toughness made the bars highly susceptible to failure when subjected to high stresses.

- **What's the chain of action that led to the failure?**

The chain of actions leading to the failure involved the following steps:

1. The prestressed steel bars were subjected to high levels of internal stress during the prestressing process.
2. Small surface cracks, which were present in the bars, acted as stress concentrators.
3. Under the combination of internal stresses and external loads, the stress intensity at the crack tips exceeded the critical stress intensity factor (KIC) of the bars.
4. As a result, brittle fracture occurred at the locations of these surface cracks, leading to the failure of the bars.

The presence of the surface cracks and the low fracture toughness of the bars were the critical factors that initiated and propagated the failure, emphasizing the importance of damage tolerance in the design and use of prestressed bars.

C. Ruling out alternate failure mechanisms**• Can plastic deformation be ruled out? If yes, explain how.**

Yes, plastic deformation can be ruled out as the primary failure mechanism. The article discusses the use of Linear Elastic Fracture Mechanics (LEFM) to analyze the failures. LEFM is a theory that primarily applies to brittle materials and is not suitable for analyzing plastic deformation. Additionally, the fact that the stress-strain curve and behavior of the bars are consistent with brittle failure supports the exclusion of plastic deformation as the primary failure mode.

• Can creep be ruled out? If yes, explain how.

Creep can be ruled out as the primary failure mechanism based on the type of loading and the nature of the failure. Creep typically occurs over an extended period under sustained loads, and the failures discussed in the article occurred during the stressing of the bars, which is a relatively short-duration event. The brittle nature of the fracture and the use of LEFM for analysis further suggest that creep was not the primary cause of failure.

• Can brittle fracture be ruled out? If yes, explain how.

Brittle fracture is not ruled out; in fact, it is identified as the primary failure mechanism. The analysis in the article, including the fracture toughness measurements, stress intensity factor calculations, and the appearance of fracture surfaces, all point to brittle fracture as the primary mode of failure.

• Can fatigue be ruled out? If yes, explain how.

Fatigue can be ruled out as the primary failure mechanism because the article describes that the bars were subjected to high loads during the prestressing process and failed during this process. Fatigue failure typically occurs under cyclic loading, and in this case, the loading was not cyclic but rather a one-time application of high stress during prestressing. The fracture morphology and behavior were also consistent with brittle fracture, not fatigue.

• Can environmentally assisted failure be ruled out? If yes, explain how.

Based on the information provided in the article, environmentally assisted failure is not ruled out or explicitly discussed. The focus of the analysis appears to be on the mechanical properties and fracture mechanics of the bars. Environmental factors such as corrosion or chemical exposure are not mentioned as contributing factors to the failures. However, without specific information regarding the environmental conditions, it's challenging to definitively rule out environmentally assisted failure as a potential factor.

D. Recommendations to prevent similar failures in the future**• How should the design, material, use, etc. be developed to avoid similar failures in the future? Provide several alternatives and indicate most promising.**

Some recommendations are:

- Improved Material Selection: Consider using prestressed steel bars with higher fracture toughness. This would increase the damage tolerance of the bars and reduce the susceptibility to brittle fracture.



- Enhanced Quality Control: Implement rigorous quality control measures during the manufacturing and handling of prestressed bars to minimize the presence of surface defects, such as cracks or other imperfections.
- Regular Inspection and Testing: Establish a regular inspection and testing regimen for in-service prestressed bars to detect any surface defects or damage early. Non-destructive testing techniques, such as ultrasonic testing, can be used to assess the integrity of the bars.
- Design Modifications: Consider design modifications that reduce the stress concentration at potential crack sites. This could involve changes in the geometry of the structural elements or the use of stress-relieving features.

100603611

Materials safety: article exercise

You are working as a materials expert in your organization and your responsibility is to guarantee safe and efficient use of materials in your facility. One day, a failure in similar facility is brought to your attention, and you need to investigate the possible implications this failure has for your facility. Your job is to interpret and analyze the given failure report and to write a report, which will allow others in your organization to understand the key developments and causes leading to the failure and the necessary actions for prevention of such failures.

Read the given article and analyze the failure. Describe, how the deformation and failure mechanisms presented during the course are reflected in the case and establish the chain of actions leading to the failure. The report should work as an introductory material to your team; it should not be very long but it should enable other team members to understand the key features of the failure without reading the failure report itself.

In addition to establishing the primary cause of the failure, show why alternate failure mechanisms can be ruled out. Some failure mechanisms have not been discussed in the course yet. Conduct the analysis using your present knowledge on the subject.

If the author of the failure analysis has, in your view, neglected to address some aspects of the failure, you may indicate this in your report and suggest tests or actions that should have been done to clarify the issue.

Prepare your response by editing this word document and export it as PDF. The file name identifies you and the article. Do not change the file name (other than the extension to pdf). E-mail the pdf to "materials.safety@iikka.fi".

You may use the question list below to guide you in your analysis:

A. Description of investigation methods applied

- What means of investigation were used in the failure analysis?

Because it was noted that the fracture was caused by a surface crack, in addition to the brittle behavior of the fracture surface, linear elastic fracture mechanics was seen as simplest tool to analyze the failure.

The fracture toughness of the bars were measured according to ASTM E 399 and ASTM E 1304 standards.

The samples were extracted from the bars, making the crack plane transversal to the axis of the bar, so that the propagation plane of the samples would be also same than in the failed bars.

The rupture load as a function of crack depth was also studied and results were compared to the theoretical predictions and failure data.

In addition, it was studied, how the failure shape can affect to the local stress in the tip of the crack, pit or notch.

- What computational methods were used?

The ASTM E 399 and ASTM E 1304 are assumed to include testing machine with computer included, therefore they can be considered as partly computational testing methods. Computational tools have been used also to measure and illustrate the load vs COD values, in addition to measure and illustrate the effect of crack type to the stress concentration on its tip.

In addition, scanning electron microscopy was used for examination of the fracture surfaces.

- What material or results were obtained?

From the fracture toughness tests according to ASTM E 399 and ASTM E 1304, the results were almost same. The scattering of the toughness values were also small.

The toughness values of the test specimens according to ASTM E 399 were 32, 33 and 33 MPa m^{1/2} while they were 35, 35 and 36 in case of the ASTM E 1304 short bar specimens. Values between 33-35 MPa m^{1/2} indicate from brittle behavior. Also, additional load vs COD test results supported the brittle behavior supposition.

The load-COD results showed typical behavior of notched samples. The behavior of the samples showed quasi-stable brittle fracture, in which the energy absorption is nearly constant.

Through the experimentation related to failure geometry, it was confirmed that the fractures are much more dangerous than notches and pits, due to the higher stress concentration in the crack tip than in the tip of artificial notches used in the test.

B. The primary cause of the failure and description of the failure mechanism

- What is the primary cause of the failure (also provide reasoning)?

The primary causes for the failure were the cracks in the bar surface, in addition to the brittle behavior of the material.

The depth of the cracks in the failed bars were compared to theoretical curve about rupture load of a cracked bar as a function of crack depth. In this curve, the fracture toughness was $33 \text{ MPa m}^{1/2}$, which was close to the failed bar. The crack depth values were very close to the theoretical prediction.

The fracture toughness of the failed material was measured by following ASTM E 399 and ASTM E 1304. Results between $33\text{-}35 \text{ MPa m}^{1/2}$ indicated about brittle behavior while four out of the six results were in this region, and the two other values were 32 and $36 \text{ MPa m}^{1/2}$. The load vs COD test results were also supporting the brittle behavior supposition.

- What's the chain of action that led to the failure?

In the selection of the steel bar, the effect of the cracks to the fracture toughness may not have been considered too seriously. Surface crack have been originated to the bar at some point before or during installing it to the steel structure. The surface crack originated the fracture, when the load was applied during the building erection, even though the loads were below the scheduled working load.

C. Ruling out alternate failure mechanisms

- Can plastic deformation be ruled out? If yes, explain how.

The brittle the material the smaller is the deformation before it breaks. In this case the material was found to be brittle, which was also one of the main reasons for the failure. Therefore plastic deformation isn't a relevant failure mechanism.

- Can creep be ruled out? If yes, explain how.

The failure didn't happen in such high temperatures that it would have affected to cause failure by creep, since approx. half of the melting point is needed so that creep is significant.

- Can brittle fracture be ruled out? If yes, explain how.
- Can fatigue be ruled out? If yes, explain how.
- Can environmentally assisted failure be ruled out? If yes, explain how.

D. Recommendations to prevent similar failures in the future

- How should the design, material, use, etc. be developed to avoid similar failures in the future?
Provide several alternatives and indicate most promising.

The material of the bars should have higher fracture toughness, therefore changing the material shall be done and the safety factor shall be increased.

The quality inspections of the bars shall be arranged so that defects in the surfaces of the bars can be detected more efficiently before installation.

100542646

Materials safety: article exercise

To improve the transversal stiffness in some steel frames, post-tensioning was done with four bars set diagonally to the steel frame. Post-tensioning is used to counterbalance undesirable strains and stresses. It is done at the construction site during installation. Bars are used due to easier measurement of elongation than cables. The material used in this case was high strength steel with yield strength of 1143 MPa and tensile strength of 1285 MPa, and the elongation under max. load of 6,7 %.

Two fractures happened during post-tensioning of the bars one at about 0,3 rupture load and another at about 0,46 rupture load. Visual examination revealed that the crack was triggered by small surface crack. The crack surface showed symptoms of brittle fracture in both cases with quasi-cleavage morphology.

The fractures were analyzed with linear elastic fracture mechanics. Measurements were done in a laboratory environment with induced cracks in the materials. Fracture toughness was measured transversal to the bar axis in for same fracture plane direction as the failed bars. Scattering was small indicating brittle behavior. The measured load vs. COD (Crack Opening Displacement) shows successive failures until the broken sample is split in two halves. The energy absorption was almost instant, which is very characteristic for quasi-stable brittle fracture. When plotting the results from the laboratory tests comparing to the actual rupture load, the results match.

Although below the scheduled workload (0,6 from rupture), the material was weakened due to surface cracks. For this usage, stronger material must be selected and inspected for surface cracks. Fatigue, creep and plastic deformation can be ruled out due to clear signs of brittle fracture. The source for surface cracks is unknown. The cracks were on the bars during installation because the ruptures happened during stressing the bars.

1. Introduction, failure background, aims of the investigation

On November 25th/26th, 2005 strong south-west wind with storm force (8 Bft. \approx 18 m/s) and heavy snowfall at a temperature of approx. 0 °C were predominant in the region Münsterland, Germany. Due to these weather conditions wet snow rolls formed around the conductors of several overhead transmission lines. This led to excessive line loads of approx. 5 kg/m, [Fig. 1](#). Some of the covered conductors were sagging to the ground. Eighty-two tension and suspension towers of five different, 110 kV overhead electrical lines collapsed mostly by buckling, e.g. failed catastrophically, [Fig. 2](#). As a consequence nearly



Fig. 1. Wet snow roll with clear ice cover, diameter approx. 13 cm, line load approx. 5 kg/m. Source RWE.



Fig. 2. Collapsed deviation tension tower M65 and suspension tower M66 (appearing small in background, right). Source RWE.

250.000 people have been cut off from electrical power supply for several days. The BAM Federal Institute for Materials Research and Testing was assigned by the German Federal Network Agency (BNetzA) for the conduction of a forensic failure analysis and an assessment of possible failure causes. The task was to find out if there were other causes besides the weather conditions. Following topics had to be investigated in detail:

- Materials conditions of the specimens taken from the towers.
- Possible ageing of the transmission towers' material.
- Description of failure mechanism(s).
- Code fulfilment at the time of erection or failure.
- Sufficiency of load assumptions, in particular the assigned ice loading zone, given in former or present (time of failure) codes.

Putting it differently the aims of the investigation described in this paper were to identify the loading situation present during the disaster, which of the towers collapsed first, and which substructure in these towers failed first and if embrittlement of the steel used was one of the failure causes. Furthermore, one crucial task was to give recommendations for the prevention of similar disasters. Based on these recommendations the authority BNetzA issued new requirements [1]. Contrary to other publications such as [2] or [3], the aim of this investigation was not to predict the failure under given loads by numerical calculations. The intention was a proof (combined analytical-experimental) of an evident failure by derivation of the corresponding loading (from picture information) and determination of the reduced load carrying capacity of structural parts.

Brittle fractures are not characteristic for this type of mild structural steel. Pohlmann [4] described brittle fractures of diagonal members and corner rods he found analysing in service failures of transmission towers in Europe. Helms et al. [5] investigated the failure of a transmission tower of the german railways and found out, that embrittlement is localised around the stamped holes of steel profiles made of Thomas steel, compare Sections 2.3 and 2.4.

Latest publications regarding failure analyses of transmission towers describe the simulation techniques used for structural failure prediction in order to avoid expensive full scale tests of transmission lattice towers [2,3] or transmission poles [6]. Moon et al. [7] carried out sub-assemblage test of a half-scaled transmission tower to estimate its performance against wind loads and compared the experimental results with those of numerical analysis. Forensic analyses like those on failures of wind turbine towers [8,9] have not been published for transmission tower failures until now.

2. Failure investigation and results

2.1. Failure site inspection

During a visit of the failure site in the western region of Münsterland eleven of the failed electricity towers were inspected on December 20th in 2005, Fig. 3. Signs of surface corrosion were not found. A corrosion induced weakening of the structures could be excluded. Fifteen samples were taken from four of the failed transmission towers: broken diagonal members, corner rod connections and more components. The collapsed transmission tower named M65, Fig. 4, was in focus of the failure investigation based on its function as deviation tension tower, the brittle fracture of a component found there, its condition and accessibility. It was assumed, that the collapse of M65 as deviation tension tower is responsible for the failure of the supporting towers M66..M73. Moreover, an extensive photographic documentation shortly after failure has been available



Fig. 3. Failure site inspection, transmission tower M65 layed down for inspection. Searching for ruptures with brittle fracture surface.

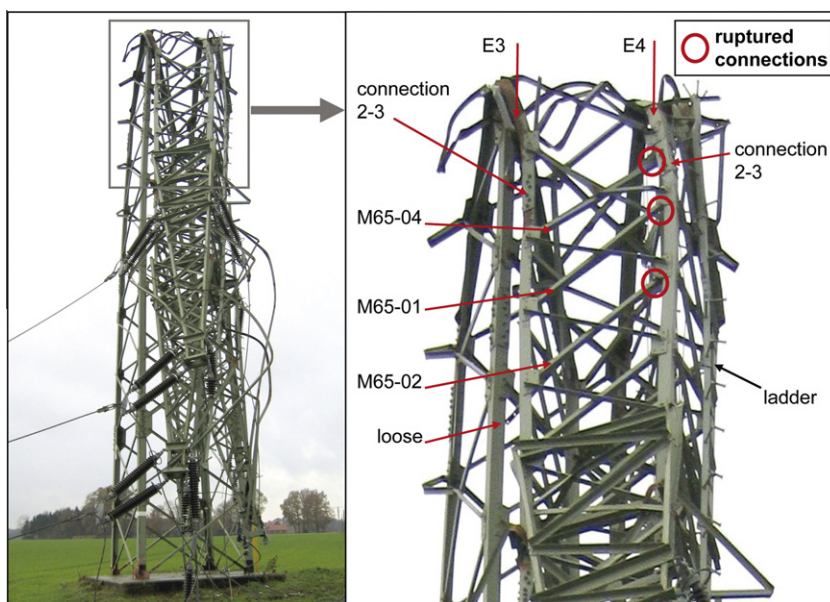


Fig. 4. Failure site inspection, transmission tower M65 in as failed position (left), Source RWE. Corner rods E3 and E4. Diagonal members M65-..., ruptures are marked (right).

for this tower, its neighbours and some more towers of this transmission line BL1503. These photos showed snow/ice rolls on some of the cables, Fig. 1, and the ice load situation at towers that did not fail. Later, more components were taken from tower M65 to be used for comparative component testing. Those were selected to be an original component, unbent and without visible damage.

2.2. Materials investigations, fractography

Materials investigations revealed that the corner rods and diagonal members of towers, that were built in the 1960's or earlier, were made of Thomas steel. The corresponding microstructure of the steel profiles close to the stamped holes showed signs of ageing in form of very small plate-like nitrides of type Fe_3N to some extent, Fig. 5. These nitrides can be etched applying Fry's reagent to the microsections. The nitrides can only be viewed in full detail using a SEM at high magnifications.

A fractographical analysis of the fracture surfaces showed that all fractures were forced fractures. Overall, no signs for fatigue failure or for corrosion induced cracking were found. The diagonal members mainly failed in a predominant brittle manner. Figs. 6 and 7 show the fracture surface of M65-4 before and after cleaning, respectively. For removing the rust warm citric acid was used at low concentration. After cleaning, the details of the fracture surfaces were analysed in the SEM. The SEM image from the centre region of the M65-4 fracture surface shows intergranular fracture, Fig. 8, whereas the image from the edges shows ductile fracture, Fig. 9. The cleaning process has generated etching pits all over the fracture surface which is the price for removing most of the rust.

2.3. Thomas steel

For a better understanding of the relations between Thomas steel and ageing as a feature of physical metallurgy some brief basic explanations are given in the following paragraphs. A recent systematic review of terms, metallurgical

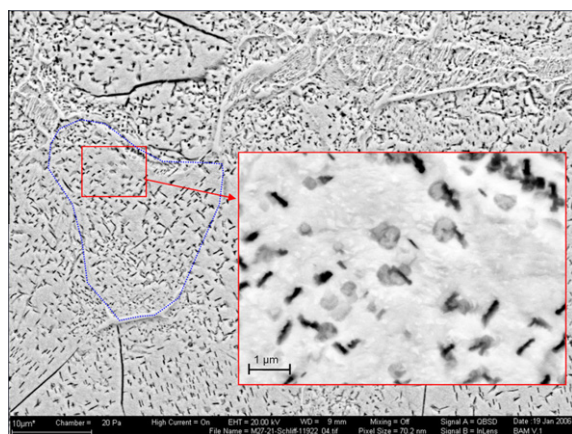


Fig. 5. Microsection of specimen M27-21, etched (Fry's reagent), SEM-micrograph: ferrite grains with nitride-precipitates. The dotted line marks a ferrite grain whose (001)-plane is perpendicular to the section plane.

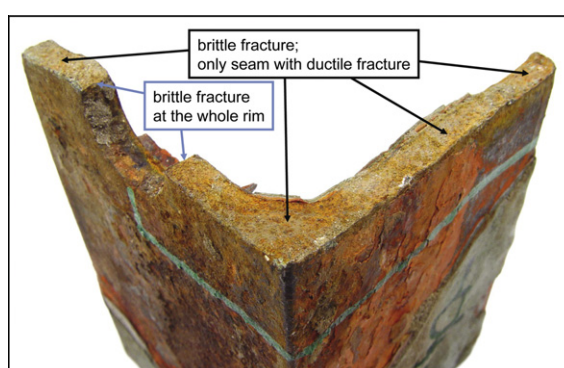


Fig. 6. Original fracture surface of diagonal member M65-04, L-profile $60 \times 60 \times 6 \text{ mm}^3$, material: plain carbon steel St 37.12 (1960), Thomas steel, mainly brittle fracture with only a few ductile areas.



Fig. 7. Original fracture surface M65-04 after cleaning. Most of the rust was removed.

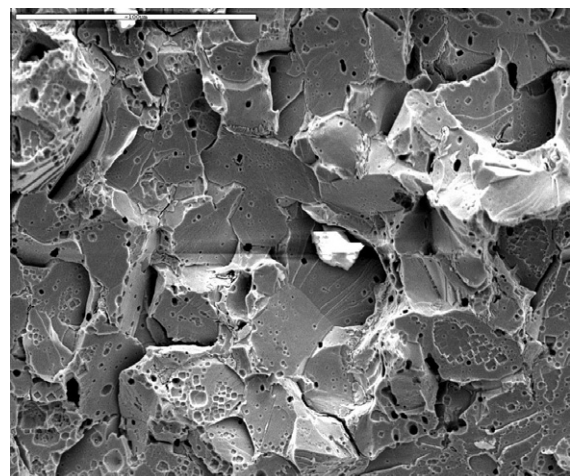


Fig. 8. Magnification of fracture surface M65-04, cp. Fig. 7, intergranular fracture with etching pits. SEM, SE mode.

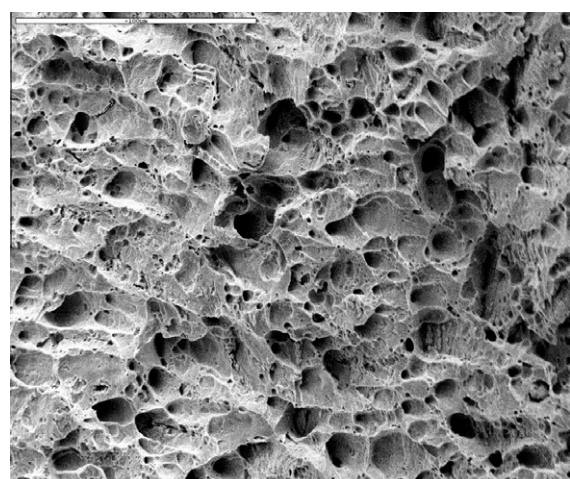


Fig. 9. Fracture surface M65-04, ductile fracture with etching pits at the seams of the fracture surface. SEM, SE mode.

background and mechanisms of ageing as well as its impact on mechanical and technological properties of Thomas steel is given in [10].

In 1878 Sidney G. Thomas and Percy G. Gilchrist introduced a method for steel making which is suitable to use iron ores rich in Phosphorus. The method is based on a basic lining of the Bessemer converter and air blasting from the bottom of the converter. Later on the method was called Thomas process and all steels produced by it Thomas steels. Over the decades, a number of technological modifications of the Thomas process had been successfully invented to improve the properties of Thomas steels. It is important to note that Thomas steels had been used very successfully and gained a remarkable economical importance worldwide. In Germany, where solely until 1943 about 300 million tons of Thomas steels had been molten [11], the production had remained over a period of about 100 years until the late 1970s. At that time the steel making by Thomas process was ceased due to technical and economical aspects.

From a metallurgical point of view, Thomas steels are typically characterized by elevated contents of Phosphorus (due to the iron ore) and Nitrogen (due to air blasting) and they are comparably low in carbon, [Table 1](#). The nitrogen content >0.01 wt.% makes Thomas steels susceptible to ageing.

2.4. Ageing of Thomas steel

Ageing is a time dependent alteration of mechanical and technological steel properties whereas two basic mechanisms are distinguished. Age hardening (quench-ageing, natural ageing) depicts the blockage of dislocations by interstitial atoms and the precipitation of embrittling nitrides and carbides in a supersaturated-iron solid solution. Ageing after a mechanical deformation is denoted strain ageing. Within strain ageing the migration of interstitial atoms to dislocations and their blockage is the predominant mechanism due to the high number of dislocations present. The blockage of dislocations by interstitial atoms as well as the complication of dislocation movement by precipitations reduce ductility and toughness of the material. Basically, both interstitial elements, nitrogen as well as carbon, take part in diffusion processes within ageing. But the major role can be attributed to nitrogen due to its higher solubility in the iron lattice and its higher diffusion rate [12–16].

Embrittlement as result of ageing may become a prime issue with respect to the assessment of the loading behaviour and safety of Thomas steel components. Outstanding examples are cut edges and stamped holes in sheet metal, plates and profiles of screwed or riveted steel structures. These material regions are exposed to significant plastic deformation which acts as prerequisite of strain ageing. In combination with a steel grade susceptible to ageing embrittlement (like Thomas steels) as well as structural stress concentration, higher stress triaxiality due to component thickness and loading features like low temperature and/or higher loading rate brittle fractures can be caused in service. Details of a corresponding failure analysis on overhead transmission line towers of Deutsche Bundesbahn are reported in [5].

2.5. Mechanical testing

In order to find out the type of steel used, standard specimens were prepared from components from tower M65, see Section 2.1, and mainly used for tensile and Charpy tests. Tensile tests were performed in accordance to DIN EN 10002-1 [17]. Tensile strength and elongation of all tested standard specimens ($R_m \sim 400$ MPa, $A \sim 37\%$) were within the tolerances of materials standards for mild steel (present and year of erection). Standard Charpy specimens ISO-V made of a diagonal member of M65 fulfilled the 27 J-criterion at 20 °C with a value of 47 J but failed at 0 °C with a value of 21 J and at –20 °C with a value of 6 J. Thus Charpy testing revealed low temperature embrittlement which still was in agreement with old material standards (DIN 17100:1957). Mechanical testing of standard specimens did not reveal any effect of embrittlement at all. This may be explained by the small volume of strain aged material around stamped holes in components, see Section 2.4, which usually is not part of the material volume of standard specimens.

For estimating the effect of embrittlement on fracture forces, component type specimens containing the original riveted or bolted connection between corner rod and diagonal member were worked out of original parts of deviation tower M65 and tested, [Fig. 10](#). The tests were performed at ambient temperature and at 0 °C and resulted in both cases in more or less brittle fractures, [Fig. 11](#). The results were in perfect agreement with previous investigations [4].

The tensile tests of the structural parts, see [Fig. 11](#) and [Table 2](#), revealed fracture forces which partly achieved only 60% of the design capacity, the estimated minimum fracture forces based on the corresponding codes [18]. This means that standard specimens without holes or notches are not suitable for the identification of Thomas steel embrittlement of components, because they did not undergo plastic deformation and ageing. Today steel for use as a construction material for transmission towers has to comply with Sxxx-JR requirements, e.g. a transition temperature ≤ -70 °C.

Table 1

Chemical composition of original members of tower M65 (built 1960). All reported values are in wt.%.

	C	Si	Mn	P	S	N
Corner rod (M65)	0.1690	<0.006	0.3680	0.0338	0.0267	0.0120
Diagonal member (M65)	0.0480	<0.006	0.4680	0.1040	0.0666	0.0160

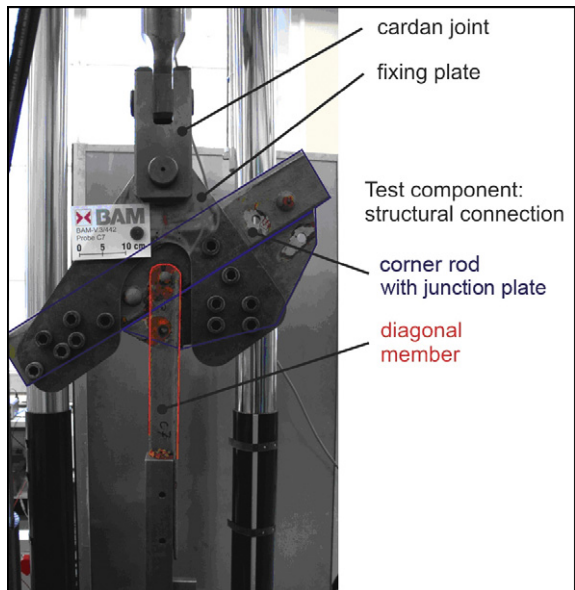


Fig. 10. Test rig for tensile testing of components (corner rod/diagonal member connection).



Fig. 11. Tensile testing of structural parts (corner rod/diagonal member connection). Brittle fracture of netto cross-section.

Table 2

Results of the tensile tests of structural parts of tower M65.

Tested component	Net cross section (mm ²)	Calc. max. force (kN)	Test temp. (°C)	Max. force during test (kN)	Deviation ¹ %
B3	444	151	23	188	25
B5	444	151	23	177	17
B4	445	151	0	185	22
A5	444	151	0	182	21
C2	464	158	23	137	n.a. ²
C1	464	227	23	155	n.a. ²
M65-07B	464	158	23	131	-17
M65-07A	464	158	23	143	n.a. ²
C3	464	158	0	158	0
C7	464	158	0	164	4
M65-01	464	158	0	170	n.a. ²
M65-08A	464	158	0	125	-21
M65-09A	464	158	0	94	-40

¹ Deviation between calculated maximum force and maximum force during test in %.

² Failure of bolt or rivet.

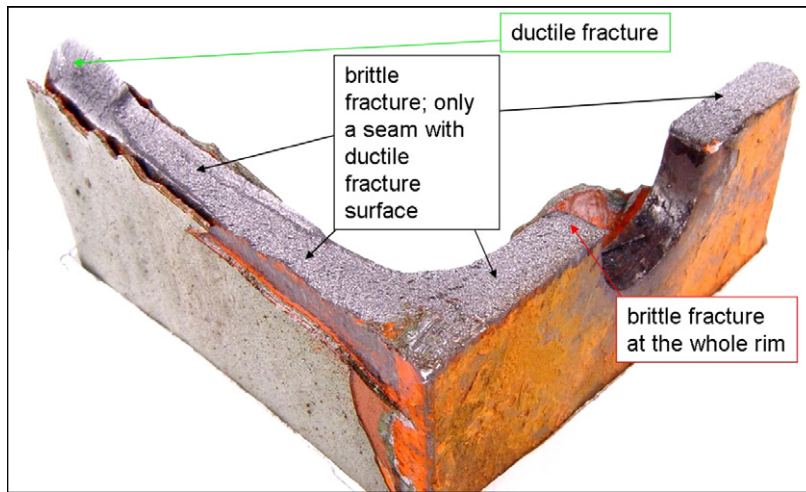


Fig. 12. Fracture surface M65-09 after mechanical tests in the laboratory. Similar fractographic appearance as the original fracture surface, cp. Figs. 6 and 7.

The fracture surfaces of diagonal members tested in BAM, Fig. 12, appeared almost identical to the original fracture surface concerning areas of brittle and ductile fracture, Fig. 6. Therefore it was concluded, that the fracture forces of the diagonal members during failure of the tower were about the value of those tested in the laboratory (94...125 kN), cp. Table 2. Consequently, these fracture forces were used in further static analyses.

2.6. Influences, failure load case

Weather conditions (snowfall, strong southwest wind) led to preferred deposition of snow on conductors of overhead electrical lines (northwest-southeast) perpendicular to dominant wind direction (southwest). Wet snow rolls with 13 cm and more in diameter formed, Fig. 1, that exceeded the line loads given in former [18] and current [19] design codes. At direction changes of overhead electrical lines specially designed deviation tension towers are used which are able to carry higher horizontal loads. During the severe weather conditions a change in line direction led to a deposition of snow rolls on the conductors, Fig. 1, perpendicular to the wind direction while in the direction parallel to the wind there were nearly no snow rolls. This applies for nearly all aerial lines that were pulled down during that night. Starting from the lines affected, it was investigated why the towers failed. Extensive photographic documentation provided by the operator (references in [20]) showed that snow rolls of the critical size were only existant at one field of deviation towers but not on the other field more parallel to wind direction. Moreover, photographs showed fields of this line BL1503 where conductors on the right side were covered with ice while they were not on the left side. This could be explained by different electrical currents of left and right electric system during snow/ice accretion. This meant for the further investigated deviation tension tower M65 that only the conductors on the right side (viewing direction towards increasing tower numbers) were covered with snow rolls while the conductors on the left side were not. This led to an asymmetric load distribution. The incoming conductors had only little snow coverage. This onesided and field-dependent (unequal) loading with lineloads of approx. 5 kg/m was identified as load case before failure of tower M65 and will be referred to as "failure load case", Fig. 13.

2.7. Load analysis

One deviation tower (M65) and one suspension tower (M66) were modelled for linear structural analysis. According to the current design code for overhead electrical lines (EN 50341-1:2001[19]) and also according to all the earlier codes (e.g. VDE0210:1958 [18]) linear analysis is sufficient. It could be confirmed that the transmission towers M65 and M66 fulfilled the code requirements (VDE0210:1958, [18]) applicable at the time of erection. The calculations clearly showed that for the forensic failure analysis further investigation should be focused on the deviation tower M65 as the suspension tower M66 is much less susceptible to increasing vertical loads respectively asymmetrical loading. From the failure site inspection (see Section 2.1) and fracture surfaces analysis (see Section 2.2) it was obvious, that rupture under tensile loads must be considered.

A "failure load case" could be derived on basis of the available information, Section 2.6, which was used to calculate the forces acting on the components prior to failure, Fig. 13. However, on site rupture was not observed for components of tower M65 showing the highest calculated tensile forces, e.g. highest utilisation factor. By comparison with experimental fracture forces of components (diagonal members) from tower M65, Section 2.5, the component showing primary failure could be identified: primary failure occurred at the joint of a diagonal member under calculated tensile force $F_{S,calc}$ of about

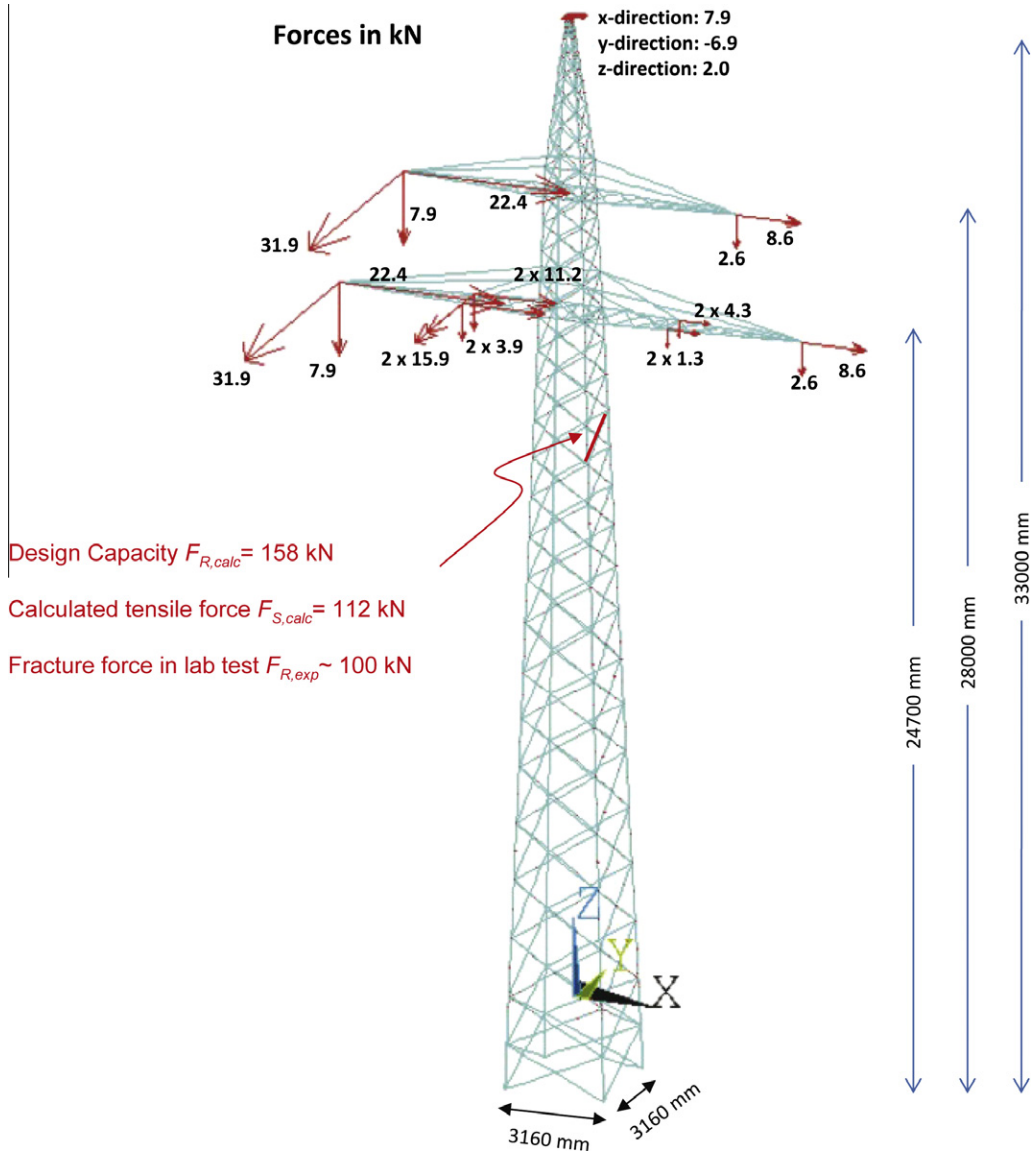


Fig. 13. FE-model of transmission tower M65, main tower dimensions, reconstructed “failure load case” with applied forces in kN and resulting loads on the diagonal member that failed initially.

112 kN, see diagonal member M65-04 in Fig. 4. This diagonal member with a L profile Section 60 mm × 60 mm × 6 mm originally had a design capacity $F_{R,calc} = 158$ kN. Its failure reason is the weakening of this member (made of Thomas steel) by embrittlement down to a fracture force $F_{R,exp}$ of about 100 kN (94–125 kN), see Section 2.5. The brittle fracture of diagonal member M65-04 occurred due to ageing and embrittlement around the stamped holes (highly stretched zone) for the rivets of the joint connecting the member and the main leg, Figs. 6 and 7. As a consequence of the rupture of the diagonal member M65-04, the neighbouring diagonals M65-01 and M65-02 in Fig. 4 ruptured in a similar way due to a subsequent sudden increase of their load. This caused an inevitably large deformation of the tower beneath the cross arms and the tower failed eventually due to lack of bracings and buckling of the main legs.

Other failure mechanisms such as stability failure by buckling of single highly stressed diagonal members, Fig. 4, were under consideration but discarded as primary failure causes since they were contrary to visual observations [20].

- [11] Dick W. Die Thomasstähle. Härtereite-Technische Mitteilungen 1943;2:100–9.
- [12] Stolte E, Heller W. Present state of our knowledge on ageing of steels. Part I. Underlaying principles. Stahl u. Eisen 1970;90:861–8.
- [13] Heller W, Stolte E. Present state of our knowledge on ageing of steels. Part II. Effects of ageing on steels. Stahl u. Eisen 1970;90:909–16.
- [14] Felix W. Investigation of natural and artificial ageing of general construction steels. Arch Eisenhüttenwesen 1965;36:35–41.
- [15] Verein Deutscher Eisenhüttenleute, editor. Werkstoffkunde Stahl. Band 1: Grundlagen. Springer Verlag; 1984.
- [16] Dahl W, Lenz E. Effect of manganese content on quench ageing and strain ageing of carbon and/or nitrogen. Arch Eisenhüttenwesen 1975;46:119–25.
- [17] DIN EN 10002-1, Metallic materials – tensile testing – part 1: method of test at ambient temperature, German version (12 2001).
- [18] VDE 0210, Vorschriften für den Bau von Starkstrom-Freileitungen (02 1958).
- [19] DIN EN 50341-1, Overhead electrical lines exceeding AC 45 kV – part 1: general requirements – common specifications, German version (03 2002).
- [20] BAM-Gutachten V.3/442, Schadensanalyse an im Münsterland umgebrochenen Strommasten, BAM Bundesanstalt für Materialforschung und-prüfung, Berlin (04 2006).
- [21] DIN EN 50341-3-4, Overhead electrical lines exceeding AC 45 kV – part 3: national normative aspects (NNA), German version (2001).
- [22] VDE-AR-N 4210-3, Test and evaluation methods for determining the load capacity of structural members made of Thomas steel in steel lattice overhead line towers with nominal voltages of 110 kV and above, German version (05 2011).
- [23] DIN EN 50341-1 VDE 0210-1, overhead electrical lines exceeding AC 45 kV – part 1: general requirements – common specifications, German version (04 2010).

887799

Materials safety: article exercise

You are working as a materials expert in your organization and your responsibility is to guarantee safe and efficient use of materials in your facility. One day, a failure in similar facility is brought to your attention, and you need to investigate the possible implications this failure has for your facility. Your job is to interpret and analyze the given failure report and to write a report, which will allow others in your organization to understand the key developments and causes leading to the failure and the necessary actions for prevention of such failures.

Read the given article and analyze the failure. Describe, how the deformation and failure mechanisms presented during the course are reflected in the case and establish the chain of actions leading to the failure. The report should work as an introductory material to your team; it should not be very long but it should enable other team members to understand the key features of the failure without reading the failure report itself.

In addition to establishing the primary cause of the failure, show why alternate failure mechanisms can be ruled out. Some failure mechanisms have not been discussed in the course yet. Conduct the analysis using your present knowledge on the subject.

If the author of the failure analysis has, in your view, neglected to address some aspects of the failure, you may indicate this in your report and suggest tests or actions that should have been done to clarify the issue.

Prepare your response by editing this word document and export it as PDF. The file name identifies you and the article. Do not change the file name (other than the extension to pdf). E-mail the pdf to "materials.safety@iikka.fi".

You may use the question list below to guide you in your analysis:

- A. Description of investigation methods applied
 - What means of investigation were used in the failure analysis?
 - What computational methods were used?
 - What material or results were obtained?
- B. The primary cause of the failure and description of the failure mechanism
 - What is the primary cause of the failure (also provide reasoning)?
 - What's the chain of action that led to the failure?
- C. Ruling out alternate failure mechanisms
 - Can plastic deformation be ruled out? If yes, explain how.
 - Can creep be ruled out? If yes, explain how.
 - Can brittle fracture be ruled out? If yes, explain how.
 - Can fatigue be ruled out? If yes, explain how.
 - Can environmentally assisted failure be ruled out? If yes, explain how.
- D. Recommendations to prevent similar failures in the future
 - How should the design, material, use, etc. be developed to avoid similar failures in the future? Provide several alternatives and indicate most promising.

Name: Nguyen Xuan Binh
Student ID: 887799

Materials Safety analysis report on collapsed electrical towers in Münsterland

Problem Overview:

The report investigated the reasons for the failure of collapse of several overhead transmission line towers in the Münsterland region of Germany in 2005, primarily due to adverse weather conditions. The event affects 250000 people who lost access to electricity, so the study tries to understand the reasons behind the failure and provides insights based on various tests. Most importantly, a concrete solution must be proposed to prevent further catastrophic events like this.

A. Description of investigation methods applied

- What means of investigation were used in the failure analysis?**

From the report, the means of investigation for the failure analysis included:

1. Failure site inspection: a visit to the failure site was conducted, where eleven of the failed electricity towers were inspected. During this inspection, signs of surface corrosion were checked, and it was determined that corrosion-weakening could be excluded.
2. Fracture Surfaces Analysis: The fracture surfaces of the failed components were analyzed. For instance, the fracture surface of the diagonal member M65-04 was examined, and it was observed that the material exhibited signs of brittle fracture.
3. Material analysis: The author studied the properties of Thomas steel used in the construction of the towers. This included understanding the relations between Thomas steel and ageing as a feature of physical metallurgy.
4. Load case analysis: The report compared the calculated tensile forces with experimental fracture forces of components to identify the component that showed primary failure.

- What computational methods were used?**

The author lists a couple of computation methods as follows:

1. Scanning Electron Microscope (SEM): The fracture surfaces were also cleaned and analyzed under SEM to gain insights into the nature of the fracture, such as intergranular and ductile fracture characteristics.
2. Linear analysis: for the towers, especially considering the codes applicable at the time of their erection (VDE0210:1958), a linear analysis was believed to be sufficient. This analysis helped confirm that the transmission towers met the code requirements at the time of their construction.
3. Comparison with experimental fracture forces: The calculated tensile forces from the derived failure load case were compared with experimental fracture forces of diagonal members from the tower, which helped identify the component that showed primary failure.
4. Force calculations: Forces acting on the components prior to failure were calculated based on the failure load case, which clarified the components under the highest tensile forces

- **What material or results were obtained?**

Main result: The main results obtained are the failure site images and failed samples, tensile testing of structural parts, materials investigations & fractography, fracture surface analysis, and load case analysis. These results provided a complete explanation for the failure mechanism and the external factors that contributed to the collapse of the transmission towers.

B. The primary cause of the failure and description of the failure mechanism

- **What is the primary cause of the failure (also provide reasoning)?**

The primary cause of the failure of the transmission towers was identified as the brittle fracture of the diagonal member M65-04 made of Thomas steel. The report mentions that brittle fractures are not typical for this type of mild structural steel. However, the embrittlement localized around the stamped holes of steel profiles made of Thomas steel was identified as a significant factor contributing to the brittle fracture. The subsequent failures of neighboring diagonal members were a result of similar brittle fractures due to the sudden increase in their load following the initial rupture.

- **What's the chain of action that led to the failure?**

The chronological order of the transmission towers' failure is as follows:

1. Initial embrittlement and brittle fracture: The diagonal member M65-04, made of Thomas steel, experienced embrittlement around the stamped holes
2. Subsequent failures: As a direct consequence of the rupture of the diagonal member M65-04, the neighboring diagonals M65-01 and M65-02 experienced similar brittle fractures.
3. Large deformation and tower collapse: The combined failures of these diagonal members caused significant deformations in the tower beneath the cross arms. Without adequate bracing to support the structure, the main legs of the tower buckled, making it collapse.
4. Consideration of other failure mechanisms: While other potential failure mechanisms, such as stability failure by buckling of single highly stressed diagonal members, were considered, they were ruled out as primary failure causes.

C. Ruling out alternate failure mechanisms

- Can plastic deformation be ruled out? If yes, explain how.

Plastic deformation can be ruled out since the failure occurred predominantly due to brittle fracture caused by embrittlement in specific areas of the tower components.

- Can creep be ruled out? If yes, explain how.

Creep can be ruled out since it is more pronounced at elevated temperatures. The failure of the towers in Münsterland occurred during severe weather conditions with snowfall, implying colder temperatures. This is not the typical environment where creep would be a failure mechanism.

- Can brittle fracture be ruled out? If yes, explain how.

No, it cannot be ruled out since it is the main reason stated in the report.

- Can fatigue be ruled out? If yes, explain how.

Probably no. The cyclic loading of the snow during the winter, while the nature of loading is stochastic in itself, can induce some fatigue on the diagonal members.

- Can environmentally assisted failure be ruled out? If yes, explain how.

Environmentally assisted failure can be ruled out since during the failure site inspection, the report mentions that signs of surface corrosion were not found on the towers. As a result, corrosion-induced weakening of the structures was excluded as a cause of failure.

D. Recommendations to prevent similar failures in the future

- How should the design, material, use, etc. be developed to avoid similar failures in the future? Provide several alternatives and indicate the most promising.

To avoid similar failures in the future, several design, material, and usage recommendations can be inferred from the paper:

1. Material Conditions: Ensure thorough inspection and assessment of the materials used in the construction of transmission towers. This includes understanding their susceptibility to embrittlement, and their performance under various environmental conditions.
2. Load assumptions: Reassess the load assumptions, especially in regions prone to severe weather conditions. The assigned ice loading zone should be reviewed to ensure that the towers can withstand the maximum expected loads.
3. Prevention of Embrittlement: Given that embrittlement of the steel used was identified as one of the failure causes, measures should be taken to prevent or mitigate embrittlement. This could involve using different materials, treatments, or design modifications.

100748275

100748275

BACKGROUND

The article reports the failure of high-power transmission lines in Munsterland, Germany. The extreme weather conditions in Munsterland Germany causes wet snow roles to be formed around the conductors of overhead transmission lines. Several tension and suspension towers of different electrical lines collapsed catastrophically. This resulted in the power supply cut for millions of people for many days. The German Federal Network Agency (BNetza) were given the task to investigate the failure of transmission lines and to find out the causes of failures other than the weather conditions.

INVESTIGATION METHODS

The federal agency took charge of the failure analysis and visited the site. The main tasks of the investigating agency were to find out the loading conditions present at the time of failure, the material used was the cause of the failure (Tomas steel in this case). They also provided recommendations to prevent future failures in similar scenarios and issued new requirements as well. The main investigation methods used by them were:

- **ON Site Inspection**

During the On-Site inspection, they found out that the transmission tower M65 was the cause of failure for the supporting towers M66 and M73 since M65 was the focus of failure investigation based on function as deviation tension tower. The photographs of the failed M65 tower are attached in the article.

The material investigations revealed that the corner rods and the diagonal members were made of Tomas Steel. Tomas steel is a steel that is named after G. Tomas and Percy G that introduced a method of making steel that uses iron ores that are rich in phosphorus. The steel making process was called the Tomas process and so the steel produced by this process as Tomas steel. Tomas steels have high phosphorous and nitrogen content, but they are generally low in carbon.

- **Fractography**

The fractographic analysis showed that the failure was due to forced fractures. The diagonal surfaces showed a brittle failure while the SEM analysis showed that the center region's fracture was intergranular. However, the image from the edges showed ductile fracture.

The microstructure of the steel profiles close to the stamped holes showed signs of ageing in the form of small plate like nitrides. These can only be viewed at high magnifications in SEM.

The next step in the investigation was to identify that did the ageing of the Tomas steel caused the failure of the transmission lines.

The agency found out that the failure could have been caused by the strain ageing phenomena in the transmission lines since there was huge mechanical deformation before failure that caused strain ageing in Tomas steels. Strain ageing reduces ductility and toughness in the

material and causes nitrogen to diffuse into the iron lattice structure because of its higher diffusion rate.

- **Mechanical Testing**

Tensile and Charpy impact tests were performed using standard samples of the M65 transmission line. Tensile test results were satisfactory and within the tolerance limits of the mild steel. Charpy specimen made out of a diagonal member of M65 failed at low temperatures of 0 and -20C with a value of 21J and 6J respectively and therefore Charpy testing revealed low temperature embrittlement.

One thing to note here is that the standard specimens without holes and notches are not suitable to prove the embrittlement of Thomas steel components because those did not experience extreme plastic deformation and ageing.

Snow rolls formed were formed on those conductor lines which were perpendicular to the direction of the wind. Since not all the conductor lines were not covered with snow, this led to an asymmetric load distribution. This one sided and unequal loading caused the failure of the M65 tower and was regarded as the failure loading case.

PRIMARY CAUSE

It was revealed during investigation that the primary cause of failure in components like stamped holes, corners and diagonal shaped members is the embrittlement of steel due to ageing. These are the locations that experience the highest amount of plastic deformation and become the prerequisite sites for strain ageing. Since Tomas steels are susceptible to embrittlement, loading features like low temperature or higher loading rate can cause brittle failures in service. The primary failure occurred at the joint of a diagonal member. This diagonal member failed due to the ageing and embrittlement around the stamped holes. The rupture of one diagonal member causes the load to increase in the neighboring diagonals causing their failure. The fracture surfaces of the materials tested in laboratory were almost same to the original fracture surface concerning the ductile and brittle fracture therefore they concluded that the fracture forces of the diagonal member during the failure of the tower were about the value of those tested in the laboratory.

ALTERNATE MECHANISMS

The investigation also found out other possible failure mechanisms that could have been the cause of the failure of the towers. One of them was stability failure by buckling of highly stressed diagonal member, but they were discarded since they were just only visual observations. The weakening of the structures leading to failure due to corrosion was also not considered and can be excluded as well. During fractography, no signs of fatigue failure or corrosion induced cracking were observed, so fatigue failure can also be excluded from the list of possible failure causes.



PREVENTING FUTURE FAILURES

Certain steel grades are prone to embrittlement because of their chemical composition and these steels when comes in contact with severe weather conditions can increase the probability of failure of even large, welded structures. To avoid similar kinds of failures in the future, a better steel grade with less phosphorous content can be used. Also, uniform loading conditions can prevent such failures and unequal and one-sided loading can cause the sudden load increase in the supporting structure and can cause failure.

572266

1 Introduction

This report reviews a failure analysis that was conducted on failed electrical transmission tension and suspension towers. As reported by the author, 82 tension and suspension towers collapsed after a storm with heavy snowfall. Consequently, this led to power outage with approximately 250 000 people without electricity.

Photos from the failure site show transmission towers being bent over into a U-shape with no obvious damage to the structure. Some towers had surface corrosion but author excludes any corrosion mechanisms that would have weakened the structures. After closer look, some diagonal bars that supports the overall structure were fractured. Corner rods as most of the rest of diagonal bars had plastically deformed and buckled. Due to weather conditions e.g., wind, snowfall, and temperature close to 0 °C, snow was able to build up on transmission lines. It was estimated that this increased line load of approximately 5 kg/meter. This snow built up as roll shape with diameter of 13 cm and covered with ice shell. Due to increased line loading, the design codes for loading were exceeded.

The tension and suspension towers were made as lattice towers in the 1960's or earlier with steel referred to as Thomas steel (St 37.12, year 1960). This steel was produced by method called 'Thomas process' to produce steel with typically elevated contents of phosphorus and nitrogen, relatively low amount of carbon. Author states that the high presence of nitrogen makes Thomas steels susceptible to ageing.

2 Investigation methods and failure mechanisms

From 82 towers, samples from four towers were collected, such as broken diagonal members and corner rod connections. One specific tower was more focused and analysed by the author. Following studies were conducted:

- mechanical tests, such as tension test and sharp impact test,
- sample preparation by etching and microscopic fractography analysis with scanning electron microscope, and
- linear structural analysis with a finite element model with computer.

By first visually inspecting the failed diagonal bars, some the inspected bars had suffered a brittle fracture with a very small areas of ductile fracture. This can be seen with two samples with a relatively smooth but porous surface while ductile fracture areas have uneven surface with clear signs of plastic deformation. These were further analysed with SEM inspection. A section viewed from the brittle fracture zone shows signs of intergranular fracture. The ferrite grains had nitride-precipitates. Author concludes that no signs of fatigue or corrosion induced cracking was found.

Mechanical tests did not confirm any effect of embrittlement. Tension test was performed according to DIN EN 10002-1 and tested at room temperature. Tension test results were within the tolerances of material standards for mild steel (results compared during testing and year erection). However, the author was not able to achieve loading nearly as close to the designed values for some components. Sharp tests however had varying results as the test samples did not fill the 27 joules-criterion when specimen temperature was 0 °C or -20 °C. The material standard (DIN 17100:1957) for this Thomas steel states a low temperature embrittlement that this impact test confirmed.

3 Failure analysis

By combining all evidence from the author's investigation, the most likely primary failure mechanism has been a brittle fracture. However, the chain reaction that led to the failure is complex.

The chain reaction seems to have started when transmission lines were overloaded due to built up snow on top of them. This created excessive load to diagonal bars, from which one eventually failed, resulting even increased load for other structural parts. Corner bars buckled and plastically deformed due to overloading.

From the conducted studies, it was concluded that the material referred to as Thomas steel (St 37.12) had nitride-precipitates that pointed towards metals tendency for aging. Aging process embrittles the steel further making it susceptible for sudden and catastrophic brittle failure. Author also points out manufacturing processes that further enhance embrittlement: some of these diagonal bars have rivet holes that most likely have been strain aged due to manufacturing of stamped holes. Overall, the mechanical test pointed that the ultimate strength of one of these diagonal bars was around 60 % lower than what was designed due to brittle behaviour.

There are still other failure mechanisms that should be addressed and possible ruled out as a possibility. Some of them are listed here:

- Plastic deformation can be ruled out as primary failure mechanism as it would be highly unlikely that the loading of the tower lines would have caused the whole structure to deform before brittle fracture of its components. The diagonal bars were significant weak spots within the structure. After the failure, some of the components (e.g., corner bars) did plastically deform.
- Creep can be ruled out. Author conducted several studies and did not find any evidence of creep. Specimen from failed parts were collected and studied that did not point to creep. Temperatures were ambient (around 0 °C)
- Brittle fracture has been suggested as the primary failure mechanism.
- Fatigue can be ruled out as it was excluded as a failure mechanism by the author. There were no signs fatigue e.g., during visual inspection of specimen.
- Environmentally assisted failures can be ruled out when these consider corrosion or temperature. Weather caused excessive loading due to built up snow on the transmission lines. Corrosion was found on the surface of structure parts. Author excluded corrosion related failure mechanisms as there were no signs that would point otherwise.

For future recommendations, both the material and structure design should be re-evaluated. The material should be selected so that the ductility is maintained even in low temperatures and after manufacturing. Aging process embrittled the material making it weaker that could be avoided by selecting other low alloy steels. Manufacturing processes must be considered to avoid effect, such as strain aging. Design of the transmission line tower must be reviewed as it must handle more weight due to built up snow. Reviewing environmentally assisted failures and loading would be wise as these will most likely be very different in the next 60 years.

1. Introduction

Spiral welded pipes are extensively used in the petroleum industry for oil and gas transport. They are made from a coiled hot-rolled steel strip with a single continuous helical weld from end to end [1,2]. This article describes examples of the spiral welded pipe failures. The spiral welded pipe for transporting oil was made from API 5L X52 steel. The pipe diameter is 720 mm with 8–10 mm wall thickness. The weld joint is a double V type. The outside and the inside welds were made by submerged arc welding with 60° welding angle. The pipe maximum working pressure is 3.8 MPa with 30–60 °C working temperature range. Although the working pressure never exceeded the maximum working pressure limitation, parts of the pipe broke catastrophically along the spiral weld (Fig. 1a).

This study was commissioned to identify factors causing pipe failure. The microstructure and microhardness of the weld metal, weld junction, heat-affected zone and base metal were considered. The fracture mechanism was identified, highlighting factors that contributed to the spiral welded pipe failure. Finally, recommendations were proposed to avoid this type of spiral welded pipe failure.

2. Methodology

Specimens were cut from the failed pipe (Fig. 1b), mounted with Epoxy, grinded with emery paper to 2000 grade, and polished. In order to observe the macrostructure and microstructure, specimens were etched in 95% CH₃OH + 5% HNO₃ solution for 14 s.

The Charpy V-notch (CVN) impact test [3] was conducted to evaluate the notch sensitivity and impact toughness of the spiral welded pipe (base metal). Specimens (5 × 10 × and 55 mm long) were cut parallel and perpendicular to the rolling direction in order to compare the toughness in different orientations; their corresponding positions are presented in Fig. 2.

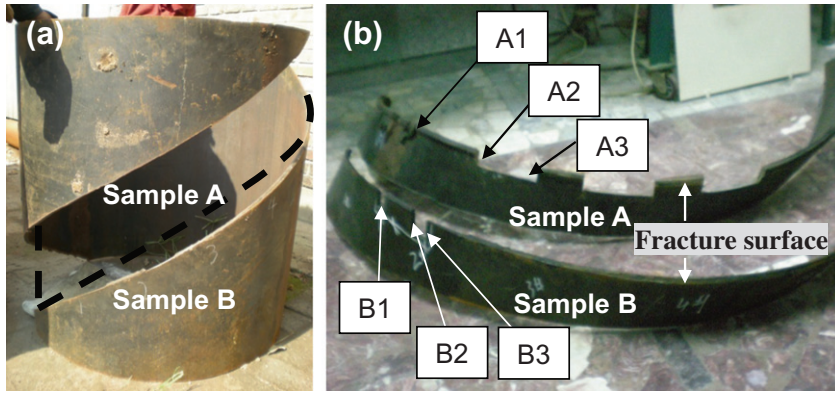


Fig. 1. (a) Fractured spiral welded pipe as received; (b) locations of analyzed specimens.

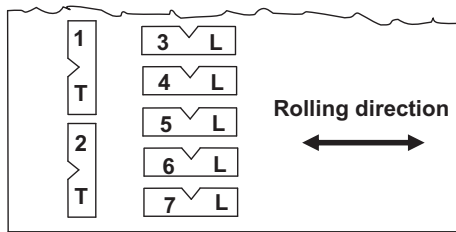


Fig. 2. Specimens for the Charpy V-notch impact test prepared in longitudinal (L) and transverse (T) orientations.

The fracture morphology and specimens' microstructure were investigated by means of optical microscopy (Leica, Germany) and scanning electron microscopy (SEM, Zeiss EVO18, Germany) equipped with energy-dispersive spectrometer (EDS). The microhardness of the welded and heat affected zones, and matrix was measured using a Vickers microhardness tester (Akashi MVK-H1, Japan).

3. Results and discussion

3.1. Failed pipe microstructure examination

Visual inspection of the etched specimens revealed that the fracture did not occur at the welding zone, but at the heat affected zone, or base metal; thus the weld was left on one fracture side, as seen in Fig. 3a and b. The spiral welded pipe microstructure is divided in three zones: welded metal, heat-affected zone (surrounding the weld), and the base metal.

In order to investigate the weld metal and the base metal compatibility, their microstructures and hardness were compared. The weld metal microstructure is lath ferrite [4] (Fig. 4a), and next to it is the heat-affected zone (HAZ). Since the heating temperature and subsequent cooling rate vary with the distance to the heat source [4,5], the heat-affected zone contains two different structures: acicular ferrite and the fine grained zone, as presented in Fig. 4b and c. Base metal exhibits fiber texture, indicating that the base metal sheets were produced by rolling (Fig. 4d). The microhardness of the weld metal, acicular ferrite zone, is HV 200, while for the fine grained zone and base metal it is HV 170. Thus, plastic deformation compatibility between weld and base metals appears suitable.

However, it was found that the base metal has low purity. Fig. 5a shows passive inclusions distributed in the base meal. A crack has nucleated at the matrix-inclusion interface (Fig. 5b). In addition, analysis by energy dispersive spectroscopy (EDS) revealed these inclusions to be iron oxide (Fig. 5b and Table 1). A number of studies [6–9] have been made on the effects of nonmetallic inclusions on the mechanical properties and fracture of alloys. Rosenfield [11] has published a thorough review of the mechanisms of initiation, growth, and coalescence of microcracks resulting from either inclusion-matrix interface separation or inclusion fracture during mechanical testing. It has been observed that the microcracks associated with inclusions can cause premature fracture and ductility. Therefore, the oxide inclusions presenting in the base metal would attribute to the pipe failure.

3.2. Failure mechanism

In order to understand the failure mechanism, fracture topography of the failed pipe should be considered. Before observing the fracture surface, the specimens were cleaned with acid pickling solution (500 mL HCl + 500 mL water + 3.5 g

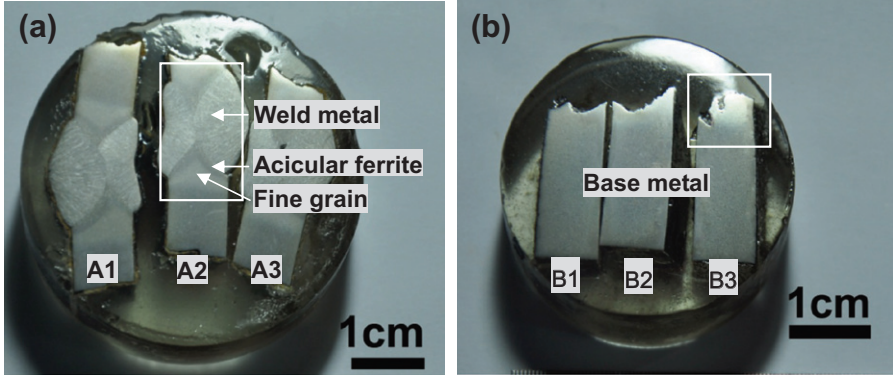


Fig. 3. Visual inspection of cross sections of fractured pipe after etching: (a) from sample A; (b) from sample B.

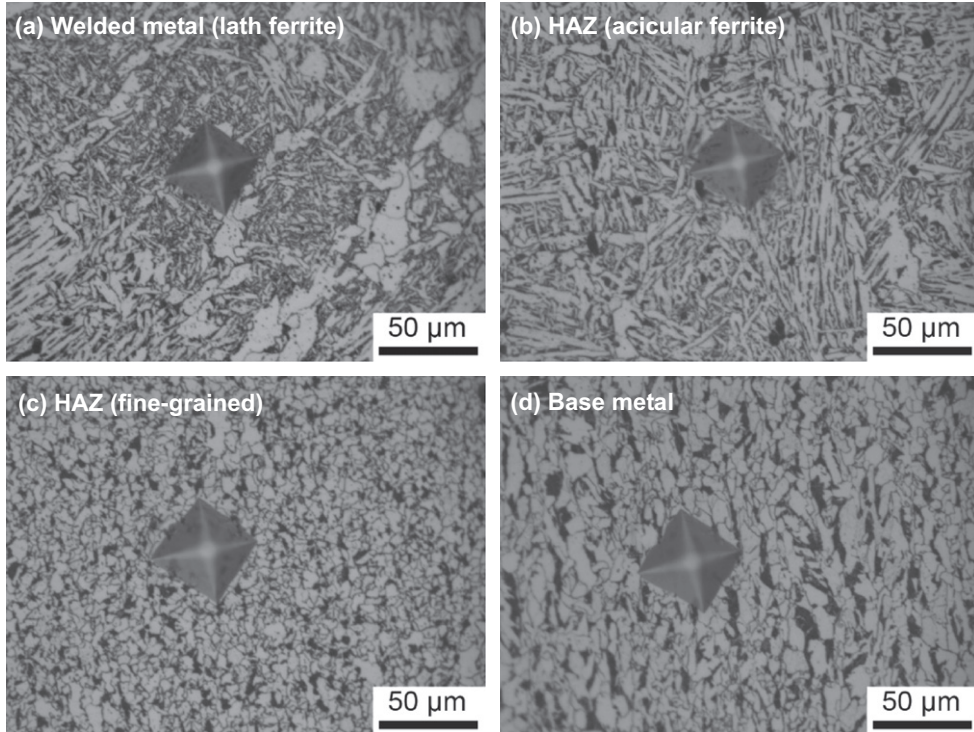


Fig. 4. Optical micrographs of cross-sections and Vickers hardness indentation of: (a) welded metal zone, lath ferrite with HV 200 hardness; (b) heat-affected zone (HAZ), acicular ferrite with HV 200 hardness; (c) fine grain ferrite with HV 170 hardness; (d) base metal with fiber texture and hardness similar to the fine-grained zone (HV 170).

hexamethylene tetramine). Cross-sectional fracture morphology was also examined, providing more information about the fracture mechanism.

SEM micrographs of the failed pipe are presented in Fig. 6a and b. Lamellar and deep groove fracture topography was observed, associated with inclusions distribution. SEM micrographs of the failed pipe cross-sections (Fig. 6c and d) contribute significantly to explanation of the pipe failure mechanism. Crack propagation is dominated by the inclusions distribution. The mechanical resistance of base metal is significantly reduced by the inclusions presence, resulting in cracks associated with inclusions. Many studies have been conducted concerning the influence of inclusions on strength and toughness reduction [6–9]. The base metal of the failed pipe is subject to significant stress concentration due to the existence of inclusions. Consequently, it is reasonable to believe that these passive inclusions are the major reason leading to pipe failure.

In order to prove that alignment of passive inclusions resulted in mechanical resistance anisotropy leading to pipe failure, the Charpy V-notch impact test (CVN, ASTM E23) was conducted. The CVN specimens were prepared with the notch in the sheet plane either parallel or perpendicular to the rolling direction (Fig. 2). The corresponding experimental data of the CVN

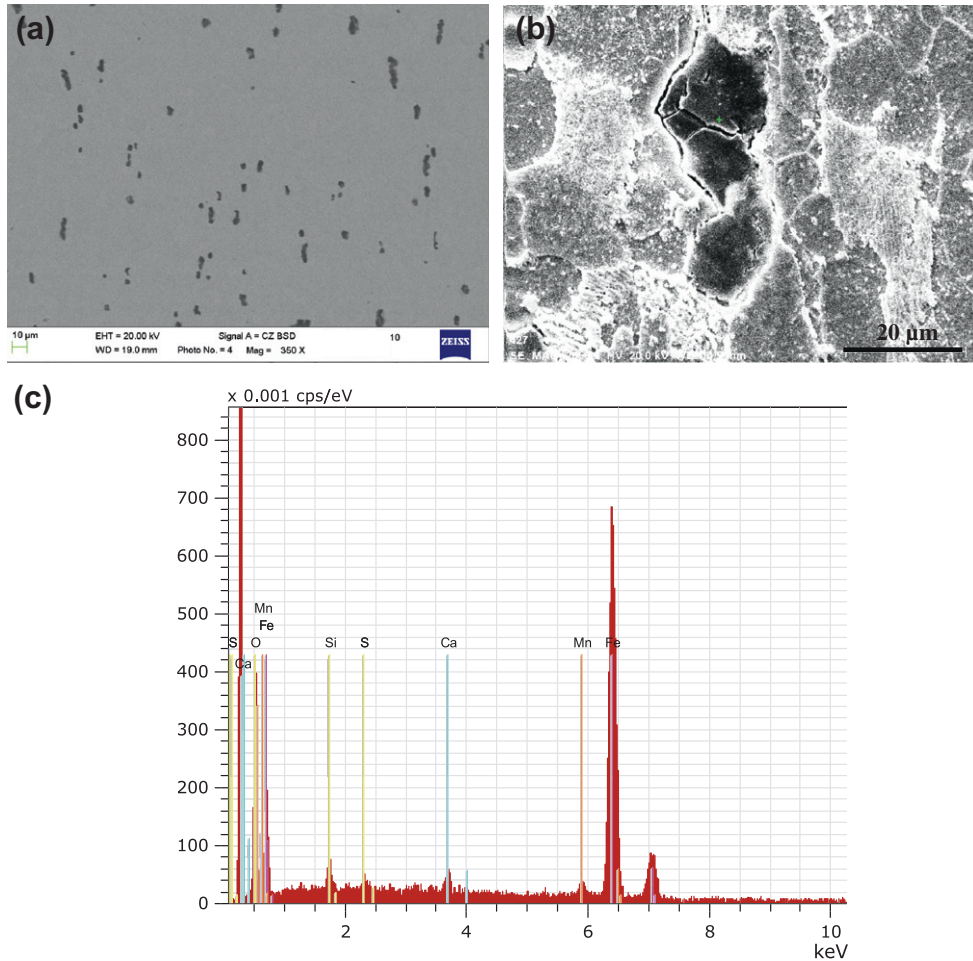


Fig. 5. (a) Distribution of inclusions in the fiber texture; (b) the oxide inclusion on the polished surface of the base metal of the pipe, (c) EDS spectrum of the oxide inclusion in (b) with, quantitative composition results shown in Table 1.

Table 1
EDS elemental analysis of the inclusions observed in Fig. 5b (at.%).

Element	Fe	O	Mn	Ca	Si	S
Inclusion	48.79	46.08	1.63	1.25	1.64	0.61

test is shown in Table 2. Longitudinally orientated specimens with respect to the rolling direction (No. 3 through No. 7) exhibited 40–44 J Charpy V-notch impact energy, while the impact energy of the perpendicular orientated samples (No. 1 and No. 2) significantly decreased to 10–12 J. SEM micrographs of perpendicular-orientated specimens (No. 1, 10 J impact energy) and longitudinally-oriented specimens (No. 4, 40 J impact energy) are shown in Fig. 7a and b. The low impact energy specimen (10 J, perpendicular orientation) exhibits deep grooves and laminate fracture topography. Ductile fracture topography in terms of dimples is associated with high 40 J impact energy for the longitudinally-oriented specimens (parallel to the rolling direction). Therefore, the CVN test revealed that due to passive inclusions aligned along the fiber texture, the base metal exhibits insufficient strength and toughness along the rolling direction. Significant cracking occurs at low stress, consequently leading to pipe failure [6].

Moreover, welding residual stress may also promote crack growth. Welding residual stress resulted from localized volume expansion. Welded metal cooling results in significant tensile stress acting on the surrounding base metal [10]. Combination of the residual stress and stress concentration promote cracks propagating along the spiral weld, finally causing catastrophic pipe failure.

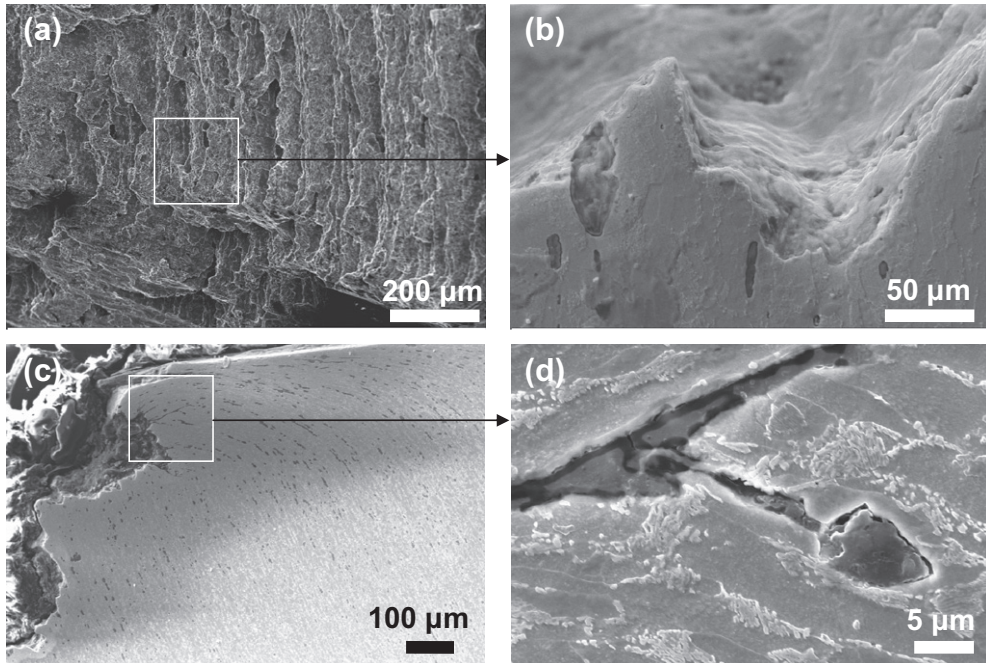


Fig. 6. SEM micrographs of the failed pipe: (a and b) fracture surface; (c and d) cross sections and material cracking associated with inclusions.

Table 2
The Charpy V-notch impact energy.

Specimen	No. 1	No. 2	No. 3	No. 4	No. 5	No. 6	No. 7
Impact energy	10 J	12 J	39 J	40 J	42 J	44 J	44 J

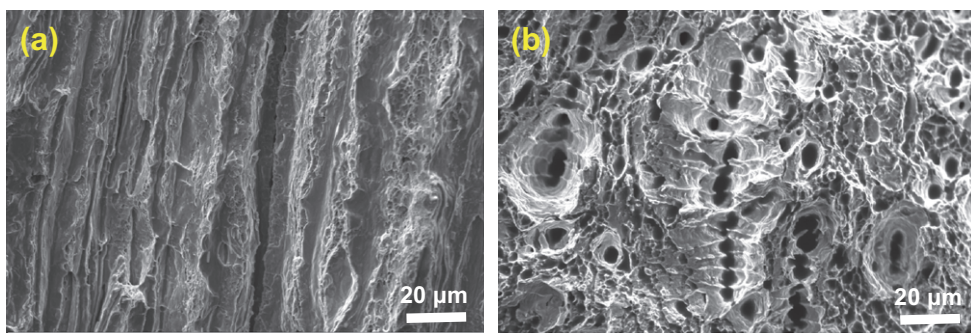


Fig. 7. The fracture morphology of the impact test specimens: (a) along the rolling direction with the Charpy V-notch impact energy of 10 J, and the fracture morphology revealing lamellar tearing; (b) perpendicular to the rolling direction with the Charpy V-notch impact energy of 39 J, and dimple fracture surface.

100509058

1 Introduction

In this report, we aim to summarize the investigation done by researchers on spiral welded pipes that failed. These pipes were made from API 5L X52 steel and had a single continuous helical welding with a double V-type welding method at a 60-degree angle. The manufacturer specified that these pipes had a working pressure limit of 3.8 MPa and could operate within a temperature range of 30 to 60 degrees Celsius. Interestingly, the research findings indicate that the failure occurred precisely along the spiral weld, despite the fact that the pipes never exceeded their prescribed pressure limit.

2 Methodology

To grasp the reasons behind the failures, the research team conducted various tests and measurements on both a macro and micro scale to gain a better understanding of the failure mechanisms.

In the macro-scale analysis, they carried out Charpy V-notch impact tests on samples taken from the pipe in two distinct orientations: one parallel to the rolling direction and another perpendicular to it. This was done to assess the toughness of the material in different directions.

In the micro-scale analysis, the research team examined the fracture surface using optical and scanning electron microscopy. The scanning electron microscope (SEM) was outfitted with an energy-dispersive spectrometer (EDS) for detailed analysis. Furthermore, they measured the microhardness in various sections of the pipe, including the welded, heat-affected, and base metal regions, using a Vickers microhardness tester.

3 Failure Causes

Similar to most failure analyses, their initial step was a visual inspection. During this examination, they noticed that the weld remained undamaged on one side of the fracture surface. Consequently, they concluded that the failure did not occur within the welded metal zone but rather in the heat-affected and base metal zones.

The microhardness analysis of various sections within the welded pipe revealed distinct microstructures. In the welded metal zone, the microstructure consisted of lath ferrite. In contrast, the heat-affected zone exhibited two different microstructures, namely acicular ferrite and a fine-grained region. The base metal's microstructure appeared as a fiber texture, confirming its production through rolling processes. The microhardness measurements indicated that the weld metal and the first heat-affected zone (acicular ferrite) had a hardness of HV 200, whereas the second heat-affected zone (fine-grained) and the base metal had a hardness of HV 170.

Scanning electron microscopy (SEM) imaging of the base metal revealed its low purity. Distributed passive inclusions were observed within the base metal. Additionally, at high magnification, it was revealed that a crack had been initiated at the inclusion-metal interface. The EDS analysis demonstrated that the inclusions were primarily composed of iron oxide. Prior research has indicated that these inclusions have the potential to generate microcracks in the metal and lead to premature fracture and a loss of ductility. Therefore, in this specific case, it was stated that the inclusions could be a contributing factor to the failure.

SEM imaging of the fracture surface indicated that the inclusions' distribution primarily governed the propagation of cracks. This was ascribed to the reduction in the mechanical strength of the

base metal due to the presence of these inclusions, leading to the initiation and spread of cracks.

The Charpy V-notch impact test on cut specimens revealed significant differences in impact energy between specimens cut in different directions. Specifically, for longitudinally oriented specimens, the measured impact energy ranged from 40-44 J, whereas for perpendicular-oriented specimens, it ranged from 10-12 J. Consequently, it was suggested that because the inclusions aligned with the fiber texture of the base metal, it exhibited inadequate strength and toughness along the fiber direction, or, in other words, the rolling direction.

4 Conclusion

The study demonstrated that a substantial number of inclusions aligned with the rolling texture of the fiber, leading to a notable decrease in the mechanical strength of the base metal. Consequently, cracks associated with these inclusions propagated. Ultimately, the combination of welding residual stress and stress concentration facilitated the easy propagation of cracks along the spiral weld, ultimately resulting in pipe failure.

Addressing the issue of steel purity could potentially provide a solution to prevent fractures and subsequent pipe failures. Additionally, enhancing welding techniques to reduce the residual stress affecting the base metal might also lower the risk of pipe cracking.